

# Sol-Gel Polycondensation Kinetic Modeling: Methylethoxysilanes

Stephen E. Rankin, Christopher W. Macosko, and Alon V. McCormick

Dept. of Chemical Engineering and Materials Science, University of Minnesota, Minneapolis, MN 55455

*Quantitative kinetic modeling of the condensation of methylethoxysilanes  $\{(CH_3)_{4-f}Si(OC_2H_5)_f\}$  of varying functionality ( $f$ ) is needed to engineer inorganic polymers, resins, and ceramics. To that end, a kinetic model that accounts for hydrolysis pseudoequilibrium, nearest-neighbor substitution effects, and unimolecular cyclization reactions in homogeneous ethoxysilane polycondensation is presented. Condensation rate parameters are determined by fitting to  $^{29}Si$  NMR transients. Several important features become evident: (1) the success of the hydrolysis pseudoequilibrium approximation; (2) strong negative substitution effects with unusual dependence on connectivity; (3) a strong kinetic tendency for ring formation, growing with methyl substitution; (4) acceleration of condensation upon methyl substitution; and (5) destabilization of three silicon rings by methyl substitution. The first three observations are consistent with previous findings for ethylethoxysilanes, but the last two are strikingly different.*

## Introduction

Copolymerization of organoalkoxysilanes offers a promising route to materials with new or improved properties and applications (Mark et al., 1995; Schaefer et al., 1996). These materials vary widely in their characteristics: some examples included toughened rubbers, scratch-resistant hard coatings, organically functionalized glasses (e.g., with nonlinear optical activity or with enzymatic activity), pressure-sensitive adhesives, release coatings, and organically modified chromatographic packing materials. Much of the interest in these materials stems from (1) the possibility of preparing metastable single-phase inorganic/organic copolymers, and (2) novel processing allowed by low-temperature, liquid-based inorganic materials processing (e.g., coating temperature-sensitive substrates with silicates).

Despite increasing commercialization of and promise for materials prepared by this route, the outcome of a synthetic strategy cannot yet be easily predicted. The qualitative chemistry underlying the polycondensation process has been characterized, but engineers demand a quantitative link between processing conditions and polymer microstructure for equation-based materials design and process control. Also, several semiquantitative hypotheses about trends in hydrolysis and condensation reactivity (and the implications of these trends) remain to be quantitatively tested [some issues are reviewed by Brinker and Scherer (1990) and by Šefčík and McCormick (1997a)]. Previously proposed models do not yet allow one to

predict sensitivities to or optimal values of even single process parameters (e.g., water content or timing of reagent addition) (notably, Re (1992) did assess qualitatively the effects of processing conditions on an ideal polycondensation model of multicomponent sol-gel polymerization—we will discuss the shortcomings of such models below).

For instance, by appropriately adjusting the ratio of mono- ( $M$ ), di- ( $D$ ), tri- ( $T$ ), and quadra- ( $Q$ ) functional silane building units, one can prepare materials ranging from Newtonian or elastoviscous fluids (silicone oils, gums) to viscoelastic or glassy solids (siloxane resins, organically modified silicates). Certain synthetic strategies have predictable results, such as limiting molecular size by terminating oligomers with  $M$  units. However, it has been shown since the earliest syntheses of these materials (Wilcock, 1947) that the ratio of  $M$ ,  $D$ ,  $T$ , and  $Q$  units alone does not allow one to predict copolymer properties. Recent studies show significant effects of the order and timing of water and monomer addition on the homogeneity and performance of silicon-based sol-gel materials (Kim et al., 1993; DeLattre et al., 1997). This needs to be put on a quantitative footing. Control of the polymer microstructure relies primarily on control of the copolymerization process itself (this is particularly true for high-molecular-weight cross-linked products and for materials generated *in situ*, where only limited postpolymerization modification (e.g., drying or pyrolysis of residual organics) is possible).

In a previous article (Sanchez et al., 1996), we quantified the effects of ethyl substitution on the polycondensation kinetics of ethoxysilanes. In this contribution, we extend this investigation to methyl substitution. Organoalkoxysilanes have seldom been studied systematically in this fashion. Schmidt and coworkers (1984) showed that replacement of ethoxyl groups with methyl groups accelerates hydrolysis under acidic conditions. Smith (1986) showed an analogous effect for methoxysilanes. Hook (1996) and DeLattre and Babonneau (1994) qualitatively surveyed the hydrolysis and condensation kinetics of several organyl- (including methyl-) ethoxysilanes. In this article, we identify *quantitative trends* in polycondensation rate coefficients.

We will begin by qualitatively describing the development of the mathematical model that we hypothesize is sufficient to match early-conversion behavior of methylethoxysilanes. Since condensation reactivity in the proposed model depends only on local connectivity of the reacting sites, we will use  $^{29}\text{Si}$  nuclear magnetic resonance (NMR), which gives local connectivity information and limited cycle-membership information, to characterize the system. We will verify our hypothesis in the Results section by fitting our model with confidence to measured  $^{29}\text{Si}$  NMR data. This will provide the kinetic parameters that are the basis of the subsequent discussion.

Under the conditions of this investigation, we will demonstrate strongly autodecelerating condensation for methylethoxysilanes. Also, methyl substitution will be shown to accelerate condensation, in contrast to ethyl substitution (Sanchez et al., 1996). This trend cannot be explained by electronic inductive effects alone. We will also show that the tendency to form four-membered rings, while strong for all systems, decreases in the order dimethyldiethoxysilane > methyltriethoxysilane > tetraethoxysilane. Finally, in contrast to observations for diethyldiethoxysilane (Sanchez et al., 1996), the three-silicon ring formed from dimethyldiethoxysilane will be shown to be unstable under these conditions.

## Modeling

### Nonideal polycondensation

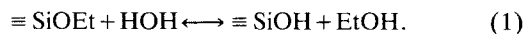
Many nonlinear polycondensation systems are well described by random-branching theory. The principal axiom of this theory states that prior reactions at a site and at its neighbors do not affect the reactivity of remaining functional groups at that site. This assumption permits the derivation of analytical expressions for the evolution of polymer structure with a minimal number of kinetic parameters (Dotson et al., 1996).

Though applying random-branching theory to hydrolytic polycondensation of ethoxysilanes would be attractive (Pepas et al., 1988; Klemperer and Ramamurthi, 1990), nonidealities unfortunately abound. Strong nearest-neighbor (or first-shell) substitution effects, cyclization, and reversibility play key roles in the development of siloxane structure (Chojnowski et al., 1977; Assink and Kay, 1988b; Doughty et al., 1990; Ling, 1992; Brunet and Cabane, 1993; Kelling et al., 1994; Ng et al., 1995; Brus et al., 1996). In this article, we incorporate known nonidealities into a quantitative model for homogeneous ethoxysilane polymerization.

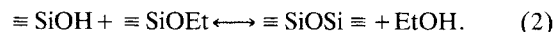
Here, we describe only the qualitative features of the

model; the Appendix outlines the full set of modeling equations. On a local level, just three (in principle reversible) reactions describe ethoxysilane polymerization:

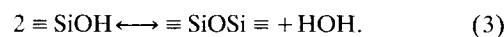
Hydrolysis:



Alcohol-Producing Condensation:



Water-Producing Condensation:



The kinetic nonidealities, though, lead to complex changes in apparent reactivities of these localized reactions as the polymerization proceeds [see, for instance, Brus and Kotlík (1996)]. As a result, many careful quantitative kinetic studies of ethoxysilane polymerization (Grubb, 1954; Lasocki, 1963, 1964a,b; Assink and Kay, 1988a) have been limited to such early reaction times that modeling equations remain analytically solvable with the use of simplifying conditions such as complete hydrolysis of ethoxyl groups, water-limited hydrolysis, and monomer consumption only by dimerization. In some cases, model compounds have been used to study specific hydrolysis rates and specific condensation rates individually (Guibergia-Pierron and Sauvet, 1992; Helary and Sauvet, 1992; Kaźmierski et al., 1994). The models used in these studies are, of course, perfectly correct, but applicable only to data in a short initial conversion range.

With the development of inexpensive numerical integration and optimization methods, investigators have begun to investigate the hydrolytic polycondensation of alkoxysilanes more fully by applying nonideal polymerization models. As a first effort, it was shown that there are first shell substitution effects (FSSE) (Pouxviel and Boilot, 1987; Smith, 1987; Assink and Kay, 1988b; Brunet and Cabane, 1993). Pouxviel and Boilot (1987) first suggested that the hydrolysis reaction of each site and the condensation reaction of each pair of sites be treated as kinetically distinct (as in Appendix Eqs. A1–A3), where the sites are distinguished by their degrees of hydrolysis and of connectivity. At around the same time, Smith (1987) recognized that rapid, complete hydrolysis of ethoxyl groups (i.e., the degrees of hydrolysis of all sites reaching constant, maximum values) allows one, independent of hydrolysis transients, to quantify the effect of connectivity on condensation reactivity.

### Hydrolysis pseudoequilibrium

Studies of hydrolysis and esterification further simplified the problem. Several reports indicated that conditions can be chosen such that hydrolysis reactions proceed for some time before significant condensation reactions begin (Wood and Rabinovich, 1989; Chojnowski et al., 1990; Sanchez and McCormick, 1992a; Chambers et al., 1993; Cihlár, 1993; Fyfe and Aroca, 1995). More recent studies have also demonstrated rapid redistribution of silanol groups as ethoxyl groups are introduced under acidic conditions (Alam et al., 1996a; Prabakar and Assink, 1997). Quantitative studies have shown

that both hydrolysis and esterification-rate coefficients can exceed condensation-rate coefficients by at least an order of magnitude (Chojnowski et al., 1990; Sanchez and McCormick, 1992a). All of these observations can be explained consistently and put to use in modeling by proposing that hydrolysis (Eq. 1) reaches pseudoequilibrium (Sanchez and McCormick, 1992b; Rankin et al., 1998a).

To estimate and compare condensation reaction rate constants, we have demonstrated the success of this pseudoequilibrium approximation (Ng and McCormick, 1996; Rankin et al., 1996; Sanchez et al., 1996). [Ling (1992) used a related approach to study tetraethoxysilane condensation rates, but assumed *a priori* a linear free-energy relationship between the rate coefficients. Such a relationship does not hold in the conditions studied here (*vide infra*).] One can *measure* the average number of silanols on *each* silicon site using  $^{29}\text{Si}$  NMR spectra (at least until peak crowding precludes accurate peak assignment). Without need to describe hydrolysis kinetics using differential equations, one can treat these values as data input into a polycondensation model with FSSE. This approach simplifies the modeling equations, reduces computational requirements (Maas and Pope, 1992), and most importantly allows robust determination of condensation rate constants. It also generalizes the approach of Smith (1987) by not requiring that hydrolysis be driven to completion.

### Cyclization

While a random-branching model with FSSE can match the silicon connectivity distribution up to fairly high conversions (Sanchez et al., 1996) [to fit site connectivity transients at high conversions, Vainrub et al. (1996) found that they needed to introduce an arbitrary time function (probably to correct for the kinetic effects of cyclization) to the rate coefficients in their FSSE-only model, although the data were well fit on a conversion scale], such a model cannot account for other information available from silicon NMR, and hence is unsuitable for structure prediction. The most obvious omission of this model is cyclization. Specific peaks in  $^{29}\text{Si}$  NMR spectra indicate that sites become involved in three- and four-silicon rings (Marsmann, 1981; Kelts and Armstrong, 1989). Sanchez and McCormick (1994) demonstrated very fast cyclization of the linear trimer, octaethoxytrisiloxane, formed during tetraethoxysilane polycondensation. Small rings also form in high yield in difunctional siloxane preparations (Barry and Beck, 1962; Clarson and Semlyen, 1993). Trifunctional silanes generate silsesquioxanes ( $\text{RSiO}_{3/2}$ ), which frequently contain polycyclic cage-like structures (Baney et al., 1995). These silsesquioxanes may form as unwanted byproducts during methyltriethoxysilane condensation in ethanol at low pH (Zhang et al., 1995).

Ng et al. (1995) have demonstrated that the bond conversion at gelation exceeds 80% for a variety of tetraethoxysilane systems. Similarly, the conversion at gelation exceeds 90% for colloid-containing silicic acid systems (Tang et al., 1993). The maximum conversion at gelation predicted with only FSSE is 50% (and that only if branching were strongly disfavored) (Bailey et al., 1990). Strong preferential cyclization has been invoked (but not quantified) to explain the inability of random-branching models to predict the gelation behavior of equilibrated *M/D/T* resins (Wilcock, 1947), the

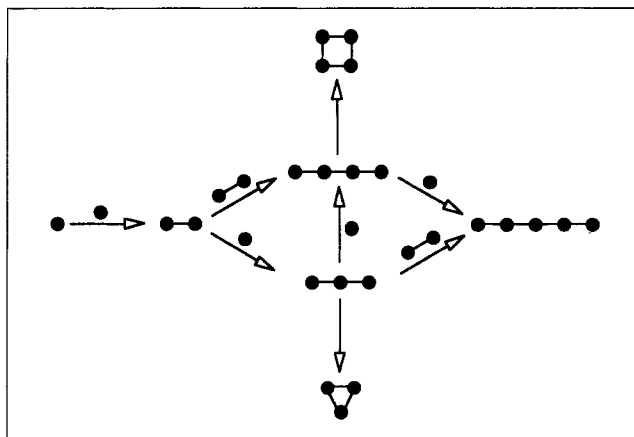
oligomer distribution during TEOS polycondensation (Brus et al., 1996), and the gelation behavior of TEOS systems (Ng et al., 1995).

### Current model

To address the kinetics of cyclization, Ng and McCormick (1996) proposed Scheme 1. This scheme includes both bimolecular and unimolecular reactions (to produce a limited set of linear chains and cyclic species). Because a limited number of species are represented, though, it can only be used for conversions of less than 40%. To build upon this scheme, we propose combining the features of the FSSE model and this molecular scheme.

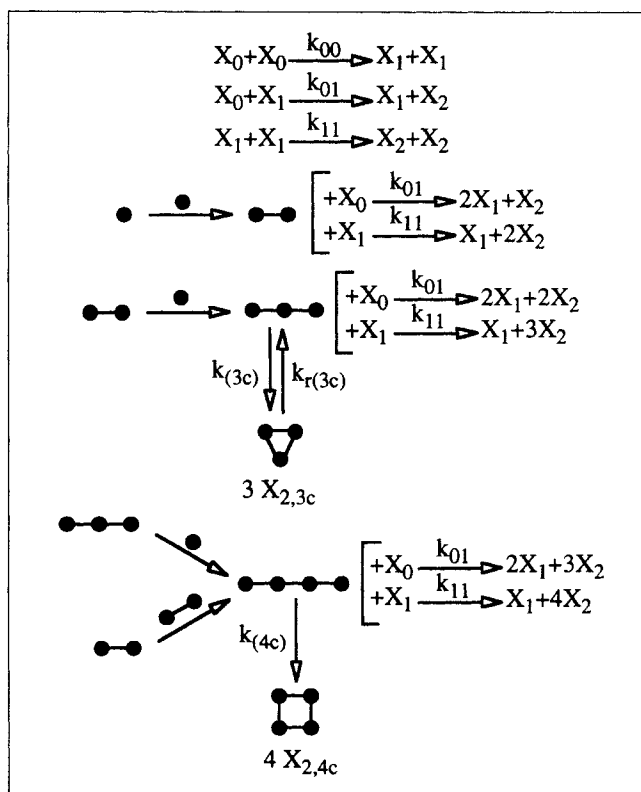
Scheme 2 illustrates the new polycondensation model, starting from a polyfunctional monomer. The model assumes hydrolysis pseudoequilibrium, which eliminates hydrolysis transients and allows us to focus only on condensation behavior. At the top of Scheme 2 is the FSSE model for sites  $X_i$  of type  $X \in \{D, T, Q\}$  and of connectivity  $i$  (note that a superscript in this notation would denote the number of hydroxyls attached to a site). A general FSSE is allowed by defining a different bimolecular rate coefficient ( $k_{ii'}$ ) for each pair of sites. In addition to these site-level reactions, we also model the formation of three- and four-silicon rings. To do this, a limited set of molecular species (dimer, trimer, and tetramer) are explicitly represented at the bottom of Scheme 2. Specific reactions are needed to model the formation of these species, but they are consumed by bimolecular reactions with any other site in solution or by unimolecular cyclization.

Once trimers and tetramer concentrations are known, unimolecular reactions can be formulated. In principle, there are infinitely many ways to form cycles, but Ng and McCormick (1995) showed that great strides are made by considering the very first possibilities—closure of linear trimers and tetramers leading to the formation of  $X_{2,3c}$  and  $X_{2,4c}$  sites in three- and four-silicon rings. While accounting for the unimolecular formation of small rings, this quasi-molecular model retains the advantages of the previous FSSE model (Sanchez et al., 1996) of not arbitrarily limiting molecular size. Only the size



**Scheme 1. Condensation reaction scheme of Ng and McCormick (1996).**

A limited set of linear and cyclic oligomers are included. Here, points represent silicon sites and lines represent siloxane bonds between them.



**Scheme 2. Condensation scheme used here.**

Both bimolecular reactions between pairs of sites and unimolecular reactions are included. Bimolecular rate coefficients ( $k_{ii'}$ ) are assumed to depend on the connectivities ( $i$  and  $i'$ ) of the two reacting sites only. The scheme shows only reactions before branched ( $X_3$ ) sites appear.  $X_i$  refers to a site with  $i$  siloxane bonds to other sites, and specific oligomers are represented by point/line drawings as in Scheme 1.

of rings formed is limited. This may seem less rigorous than statistical approaches [such as cascade theory (Gordon and Temple, 1972) or rate theory (Stanford et al., 1975)] which allow rings of any size to form, but these approaches assume Gaussian chain statistics (Stepho, 1981). Truncating the set of cyclization reactions provides more accurate polymer structure predictions than these statistical approaches (Sarmoria et al., 1990), especially when the cyclization rates do not follow those predicted with Gaussian statistics [as for polydimethylsiloxane oligomers (Chojnowski et al., 1977; Rolando and Macosko, 1987)]. The model also has the advantage of compactness (at all conversions) compared to models involving explicit rate expressions for a truncated set of oligomers (cf. Kumar and Misra, 1986).

Note in Scheme 2 that the maximum connectivity of any site is two. We intentionally omit branched sites because once they are allowed, we must account for the possibility of cyclic sites involved in branches. Because of the many possible pathways by which these sites can form, a more complicated modeling approach is needed (and is under development). Here we claim to address neither the formation of polycyclic species (such as *T*-resin cages) nor the competition between cage formation and growth of larger molecules. Understanding the kinetics of the formation of single rings is an important first step toward addressing these issues. To ensure that

the model of Scheme 2 is applicable, we only consider experimental data up to the point where significant branching (indicated by  $X_3$  sites in NMR) is first observed.

### Condensation reversibility

With one exception (the unimolecular cyclization to form the three-silicon ring), we have encountered no need to include siloxane hydrolysis (reverse-condensation) reactions. This does *not* mean that these bonds are truly irreversible—it merely means that we find no evidence of siloxane hydrolysis at a significant rate for these samples over the time considered. It is well known, though, that under acidic conditions, the *M* dimer (hexamethyldisiloxane) can hydrolyze to form monomer. Equilibrium coefficients for the *M* system ( $K_h \sim 15$  and  $K_c = [(\text{Me})_3\text{SiOSi}(\text{Me})_3][\text{H}_2\text{O}]/[(\text{Me})_3\text{SiOH}]^2 \sim 80$ ) (Šefčík et al., 1997) indicate 88% bond conversion at equilibrium for  $[\text{Si}] = 2 \text{ M}$ ,  $(\text{H}_2\text{O}/\text{Si})_0 = 2$ , and  $(\text{EtOH}/\text{Si})_0 = 4$ ; if the hydrolysis and condensation equilibrium coefficients are similar for other monomers, this is consistent with apparent irreversibility on the conversion scales observed here. Hexamethylcyclotrisiloxane is probably strained compared to larger rings (Clarson and Semlyn, 1993; Voronkov, 1996), so it should be thermodynamically more prone to siloxane hydrolysis in the absence of stabilizing influences. Note, though, that hexaethylcyclotrisiloxane seems to be considerably more stable under these conditions (Sanchez et al., 1996).

## Experimental

### Sample preparation

Table 1 lists the compositions of all systems studied here. The monomer was mixed with half of the required ethanol (Aaper Alcohol & Chemical) in one polypropylene test tube. Trimethylethoxysilane (98%), methyltriethoxysilane (99%) (both from Aldrich), and dimethyldiethoxysilane (United Chemical Technologies) were used as received. The required volumes of filtered, deionized water and a normalized (1-N) HCl solution (Aldrich) were mixed with the other half of the required ethanol in a separate polypropylene test tube. The ethanol used contained 0.0013 mol of  $\text{Cr}(\text{acac})_3$  [a paramagnetic relaxation agent for the  $^{29}\text{Si}$  nucleus (Harris, 1986)] per mole of ethanol.

We started the reactions by rapidly combining the contents of the two test tubes, closing the tube with a screw cap, and shaking vigorously by hand to mix. The starting solutions were readily miscible. An aliquot was placed in a 5-mm (OD) glass NMR tube. The tube was tightly capped and inserted into the NMR probe, which was maintained at  $23.0 \pm 0.2^\circ\text{C}$ . Spectral acquisition began within 5 min of mixing the solutions. The reaction proceeded in the NMR tube and spectra were periodically collected.

**Table 1. Compositions Included in this Study\***

Sample	$f$	$[\text{Si}]$ (M)	$[\text{EtOH}]_0$ (M)	$[\text{H}_2\text{O}]_0$ (M)	$[\text{HCl}]$ (M)
<i>M</i>	1	2.20	9.83	4.40	0.0022
<i>D</i>	2	2.24	8.96	4.48	0.0022
<i>T</i>	3	2.19	8.31	4.37	0.0023

\*The monomers used are  $(\text{CH}_3)_{4-f}\text{Si}(\text{OEt})_f$ .

## Analytical methods

We acquired  $^{29}\text{Si}$  NMR spectra on a Varian VXR-500 or a Bruker AMX-500 spectrometer using inverse gated decoupling and 8 (for *M* spectra), 32 (for *D* and some *T* spectra), or 64 (for some *T* spectra) transients per spectrum. An interpulse delay of 10 s was used to permit full relaxation of the nuclei (Sanchez et al., 1996). The total integrated intensity of all spectra remained constant throughout the measured time.

For the monofunctional system, the monomer–monomer condensation rate coefficient was found by linear regression assuming a bimolecular reaction (see the Appendix). For the difunctional and trifunctional systems, we found the set of rate coefficients providing the best fit to the experimental data with a nonlinear least-squares (Levenberg–Marquardt) algorithm. The model from the Appendix was numerically integrated at each residual function evaluation by a predictor–corrector (Adams–Moulton) method. To ensure uniqueness of the fits, several initial guesses were made and the coefficients were accepted only if all converged to the reported values upon fitting. In addition, piecewise fitting was performed to data in certain time ranges using a limited set of reactions to ensure local agreement with the data as well as a global fit.

We calculated by a semiempirical molecular orbital method the partial charges at each atom and the orders of each bond for the set of singly hydrolyzed alkylethoxysilane monomers  $\text{R}_x(\text{OEt})_{3-x}\text{Si}(\text{OH})$  ( $\text{R} = \text{CH}_3$  or  $\text{C}_2\text{H}_5$ ) and their singly protonated derivatives  $[\text{R}_x(\text{OEt})_{3-x}\text{Si}(\text{OH}_2)]^+$ , as well as for more-hydrolyzed species and dimers. Geometry optimization was performed using the MNDO (Clark, 1985) method in the MOPAC (Stewart, 1990) package. Šefčík and McCormick, (1997b) discuss in detail the choice of MNDO for silicates and the calculation procedure.

## Results

### NMR peak assignments

For the trimethylethoxysilane (*M*) system, only three sites appear, so the NMR peaks are easily assigned using their order of appearance ( $M_0^0$  decays monotonically,  $M_1$  grows monotonically, and  $M_0^1$  is an intermediate). Our assignments (Table 2) match those of Hook (1996). Note that the hydrolyzed monomer peak appears upfield of the unhydrolyzed monomer, contrasting the observed trend for TEOS (Pouxviel et al., 1987). Such a reversal in the effect of hydrolysis on chemical shift has been reported recently by Alam et al. (1996b) in the  $(\text{CH}_3)(\text{CH}_3\text{O})_i(\text{OH})_{3-i}\text{Si}$  series ( $0 \leq i \leq 3$ ).

Representative spectra for polymerizing dimethyldiethoxysilane (*D*) are shown in Figure 1a. The assignments indicated (Table 2) match those in the literature (Harris and Robins, 1978; Sugahara et al., 1992a; Hook, 1996; Lux et al., 1996). Hydrolysis again causes an upfield shift for the difunctional monomer and oligomers. Note the ease with which the cyclic trimer ( $D_{2,3c}$ ) and cyclic tetramer ( $D_{2,4c}$ ) can be distinguished by their single sharp peaks. Since these peaks are so clear and their chemical shift is insensitive to changes in solution composition, they can act as internal references (Harris and Robins, 1978). Lux et al. (1996) have reported that the chemical shifts of  $D_1^0$  and  $D_1^1$  peaks may overlap somewhat. We assumed that the minimum between the two sets of peaks in the  $D_1$  region separates  $D_1^0$  from  $D_1^1$ . This introduces some

**Table 2.**  $^{29}\text{Si}$  NMR Chemical Shift Assignments Relative to External Tetramethylsilane\*

Chemical Shift	Assignment	Chemical Shift	Assignment
<i>M System</i>		<i>T System</i>	
17.0	$M_0^0$	−38.5	$T_0^3$
14.1	$M_0^1$	−39.8	$T_0^2$
7.1	$M_1$	−41.1	$T_0^1$
		−42.6	$T_0^0$
<i>D System</i>		−47.8	$T_1^2$
−3.7	$D_0^0$	−49.1	$T_1^1$
−4.3	$D_0^1$	−50.5	$T_1^0$
−4.8	$D_0^2$	−53.8	$T_{2,4c}^0$
−8.5	$D_{2,3c}$	−56.1	$T_{2,4c}^1$
−12.5	$D_1^0$	−57.0	$T_2^0$
−13.2	$D_1^1$	−58.6	$T_2^1$
−18.9	$D_{2,4c}$	−64.3/−65.7	$T_3$
−21.3	$D_2$		

\*Average values are listed when many peaks contribute to a broad band. Notation is as in the caption of Figure 1.

uncertainty in our estimate of the average degree of hydrolysis of  $D_1$  sites, but does not affect our estimate of the total  $D_1$  site concentration.

Figure 1b shows representative  $^{29}\text{Si}$  NMR spectra collected during polymerization of methyltriethoxysilane (*T*). The peaks are assigned (Table 2) according to their order of appearance, by consulting existing literature, and by analogy with *D* and *Q* systems. The monomers ( $T_0^j$ ,  $0 \leq j \leq 3$ ) and singly connected sites ( $T_1^j$ ,  $0 \leq j \leq 2$ ) are easily assigned, but now hydrolysis results in a *downfield* shift (as happens for *Q*). Our

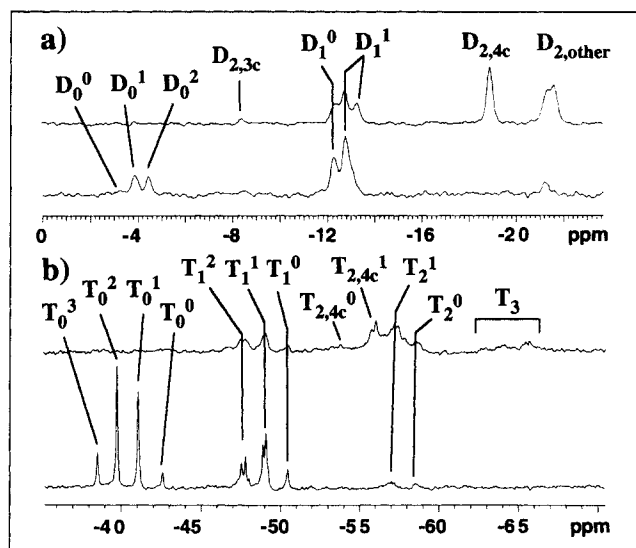


**Figure 1.** Representative  $^{29}\text{Si}$  NMR spectra for hydrolyzed (a) dimethyldiethoxysilane and (b) methyltriethoxysilane.

The lower spectrum in each case is the first acquired (after (a) 7 min and (b) 5 min) and the upper spectrum is from a later time ((a) 3 h and (b) 12 h from mixing). Subscripts indicate the number of siloxyl groups attached to the site, with “3c” and “4c” denoting sites in three- and four-silicon rings, respectively. Superscripts indicate the number of hydroxyl groups, and the remaining ligands attached to the site are ethoxyl.

assignments exactly match those of Hook (1996). Sugahara et al. (1994) demonstrated that increasing the initial water content in trimethylethoxysilane/ethanol/water/HCl solutions produces intensity changes consistent with these assignments.

To summarize the chemical shift behavior with hydrolysis observed so far, the set of methyl *M*, *D*, *T*, and *Q* ethoxysilane monomers can be divided into two categories: *M* and *D* peaks generally shift upfield as ethoxyl groups are replaced with hydroxyls, and *T* and *Q* show the opposite behavior. For all of these monomers, increasing condensation always results in an upfield shift.

Our assignments of the first  $T_2$  and  $T_3$  peaks to appear ( $T_2^j$ ,  $0 \leq j \leq 1$  and  $T_3$ ) agree with those of Hook (1996). As we follow the reaction to higher conversion, however, more  $T_2$  and  $T_3$  sites appear than Hook assigned. By analogy with *D* (Harris and Robins, 1978) and *Q* (Kelts and Armstrong, 1989) systems, the new peaks are assigned to sites in four-silicon rings ( $T_{2,4c}^j$ ,  $0 \leq j \leq 1$  and  $T_{3,4c}$ ). Notice, though, that there is an odd hydrolysis shift for the cycles. The hydrolyzed  $T_{2,4c}^j$  site is assigned *upfield* of the unhydrolyzed peak; though this is unusual for *T* sites, it is necessary to maintain the same ratio between hydrolyzed and unhydrolyzed cyclic  $T_2$  sites as for noncyclic  $T_2$  sites [as observed for cyclic and noncyclic  $Q_2$  sites (Ng and McCormick, 1996; Sanchez et al., 1996)]. This assignment (and only this assignment—all others are straightforward!) should be regarded as tentative.

No three-silicon ring peak is assigned for the methyl-*T* system. The absence of such a peak has been noted previously (Sugahara et al., 1994). Recent evidence, though, suggests that the chemical shift for three-silicon rings formed from diethylphosphatoethyltriethoxysilane lies very close to that of the corresponding  $T_1$  sites (Cardenas et al., 1996). If this is so for the methyl *T* system, it may explain our inability to detect distinct signals from these rings; if they appear, they are lost amidst several  $T_1$  peaks. We comment below on how this could affect reported rate coefficients.

### Hydrolysis pseudoequilibria

A hydrolysis pseudoequilibrium assumption pertains when forward and reverse hydrolysis reactions outpace condensation reactions sufficiently that the fractional hydrolysis conversion ( $\chi_i$ ) of sites of connectivity *i* reaches a constant value by the time a significant concentration of sites of connectivity *i* + 1 develops (Rankin et al., 1998a). Figure 2 demonstrates that for each site, the fractional hydrolysis conversion rapidly reaches and maintains a constant value before the relevant condensation occurs to a large extent. The pseudoequilibrium hydrolysis conversions ( $\chi_{i,eq}$ ) are summarized in Table 3. The validity of hydrolysis pseudoequilibrium allows us to isolate condensation rate coefficients for the set of methylethoxysilanes.

After a short initial transient, the concentrations of water and of ethanol (calculated using stoichiometries of reactions 1–3) hardly change at all, so we can determine individual hydrolysis equilibrium coefficients, defined as follows:

$$K_{h,i} = \frac{\chi_i[\text{EtOH}]}{(1 - \chi_i)[\text{H}_2\text{O}]} \quad (4)$$

We report the estimated values in Table 3. The uncertainties

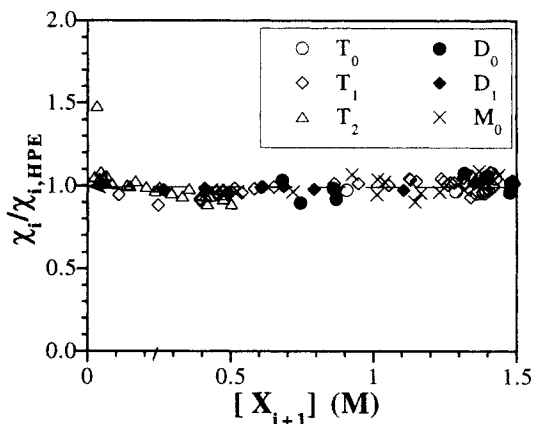


Figure 2. Hydrolysis behavior.

For each site (of connectivity *i*), the ratio of fractional hydrolysis extent ( $\chi_i$ ) to the pseudoequilibrium fractional hydrolysis extent ( $\chi_{i,HPE}$ ) is plotted as a function of the concentration of the next-most-connected site ( $[X_{i+1}]$ ). Since a value of 1 is quickly reached and maintained for all sites, hydrolysis pseudoequilibrium applies. The pseudoequilibrium fractional hydrolysis extents are listed in Table 3.

in these values come from estimating the ethanol and water concentrations from the measured site distribution data. The values all fall within the range ( $K_h \sim 10$  to 30) determined for trimethylethoxysilane at true equilibrium (Šefčík et al., 1998). The closeness of these apparent  $K_{h,i}$  values to true ethoxysilane hydrolysis equilibrium coefficients supports the hydrolysis pseudoequilibrium assumption, as we have reported for other similar systems (Rankin et al., 1998b).

### Condensation kinetics

Limiting attention to data before branched structures (characterized by  $X_3$  sites) are observed, one need not consider the many ways that cycles can become part of the polymer network. We can then quantify cyclization with the aforementioned model, in which rings do not condense further (Scheme 2). Naturally, this model is complete only early in reaction.

The fits obtained are illustrated in Figure 3. The parameters found to provide the fits shown are summarized in Table 4. As discussed in detail in the Appendix,  $\bar{k}_{w(i,i')}$  is the measured rate coefficient for condensation of a hydroxyl group on site  $X_i$  with a hydroxyl group on  $X_{i'}$ ;  $\bar{k}_{w(3c)}$  is the rate coefficient for the intramolecular condensation of a hydroxyl group on one end of a linear trimer with hydroxyl group on the other end;  $\bar{k}_{w(4c)}$  is defined similarly to  $\bar{k}_{w(3c)}$ , but for a

Table 3. Pseudoequilibrium Hydrolysis Extents ( $\chi_{i,eq}$ ) and Hydrolysis Equilibrium Coefficients ( $K_{h,i}$ ) Measured at Pseudoequilibrium for All Sites

Site	$\chi_{i,eq}$	$K_{h,i}$
$M_0$	0.81	$14 \pm 5.0$
$D_0$	0.72	$17 \pm 3.5$
$D_1$	0.65	$11 \pm 5.4$
$T_0$	0.55	$18 \pm 5.6$
$T_1$	0.63	$26 \pm 12$
$T_2$	0.60	$21 \pm 8.0$

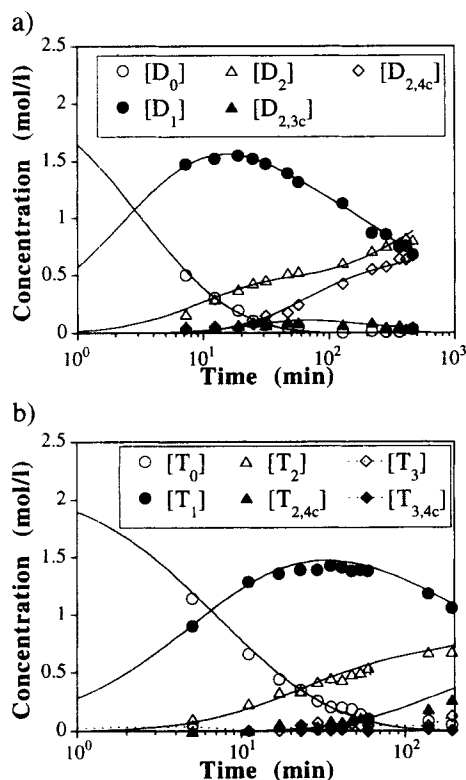


**Figure 3. Experimental data (points) and best fit of the set of kinetic equations in the Appendix (lines) for hydrolyzed (a) dimethyldiethoxysilane and (b) methyltriethoxysilane at  $23 \pm 0.2^\circ\text{C}$ .**

The parameters giving these fits are listed in Table 4.

linear tetramer; and  $\overline{k_{w,r(3c)}}$  is the rate coefficient for the hydrolysis of one siloxane bond of a cyclic trimer.

In Table 4, we report water-producing condensation rate coefficients. We also discuss all trends in terms of water-producing condensation only. Reporting the coefficients in these terms helps us both in comparing to existing literature and in comparing sites of different functionality (the rate coefficients are always expressed on a consistent basis—*per silanol*). Owing to the hydrolysis pseudoequilibrium, we cannot absolutely rule out the possibility that alcohol-producing condensation plays a role for some of these systems (Rankin et al., 1998a), but the relatively high fractional extents of hydrolysis observed favor this route (Assink and Kay, 1988a). Assink and Kay (1993) have reported alcohol-producing condensation of tetraethoxysilane to be negligible in acidic low-

water/ethanol solution. (See the Appendix for further discussion of the meaning of the reported rate coefficients if alcohol producing condensation plays a major role.)

### Three-silicon T rings

In fitting the NMR data of the T system, we first assumed that no three-silicon rings formed (giving the fit in Figure 3b and the parameters in Table 4). However, as we have pointed out already, we cannot rule out the presence of  $T_{2,3c}$  sites; they may be lumped in with the peaks we assigned to  $T_1$  sites. Therefore, we must consider whether the reported kinetic parameters would be affected by the presence of three-silicon rings.

We test the possibility of irreversible three-silicon ring closure by setting  $\overline{k_{w(3c)}}$  to various values and allowing the remaining kinetic parameters in the model to vary to fit the experimental data, assuming that the measured  $[T_1]$  is actually  $[T_1] + [T_{2,3c}]$ . We find no change either in the quality of the fit or in the estimated values of all other parameters for  $\overline{k_{w(3c)}} \leq 0.06 \text{ h}^{-1}$ . As we set  $\overline{k_{w(3c)}}$  to even higher values, the estimated values of other parameters begin to change.  $\overline{k_{w(0,0)}}$  and  $\overline{k_{w(0,1)}}$  do not change much, but  $\overline{k_{w(1,1)}}$  and  $\overline{k_{w(4c)}}$  increase significantly as  $\overline{k_{w(3c)}}$  increases. Figure 4 shows the fits and predicted  $[T_{2,3c}]$  for  $\overline{k_{w(3c)}} = 0.6$  and  $6 \text{ h}^{-1}$ . When  $\overline{k_{w(3c)}} = 6 \text{ h}^{-1}$ , the rate of change of  $[T_1] + [T_{2,3c}]$  at the highest time is predicted (because of the very high  $[T_{2,3c}]$ ) to be significantly lower than the experimentally measured rate of change (Figure 4a). We can therefore rule out this value of  $\overline{k_{w(3c)}}$  as too high. When  $\overline{k_{w(3c)}} = 0.06 \text{ h}^{-1}$ , the predicted  $[T_{2,3c}]$  significantly exceeds  $[T_{2,4c}]$ —this is unlikely to actually occur, since no such behavior has been observed for the D or Q system. Therefore, we doubt that  $\overline{k_{w(3c)}}$  is even this high.

So for all values of  $\overline{k_{w(3c)}}$  large enough to change the predicted values of the other parameters, features of the predicted curves deviate significantly from what we might reasonably expect. Therefore, we feel that the reported values of the other parameters for this system are accurate. Unfortunately, we cannot give an estimate for an upper bound of  $\overline{k_{w(3c)}}$  since, if reversibility is at play (as it is in the D system), the value of  $\overline{k_{w(3c)}}$  could actually be higher than  $0.06 \text{ h}^{-1}$  without inducing unreasonable changes in the predicted concentrations.

### Discussion

So far we have demonstrated that the proposed model is consistent with the reported early-conversion experimental

**Table 4. Rate Coefficients Found by Least-Squares Fitting of the Model in the Appendix to Early-Conversion Data at  $23 \pm 0.2^\circ\text{C}^*$**

Sample	$\overline{k_{w(0,0)}}$ ( $\text{M} \cdot \text{h}^{-1}$ ) <sup>-1</sup>	$\overline{k_{w(0,1)}}$ ( $\text{M} \cdot \text{h}^{-1}$ ) <sup>-1</sup>	$\overline{k_{w(1,1)}}$ ( $\text{M} \cdot \text{h}^{-1}$ ) <sup>-1</sup>	$\overline{k_{w(3c),r}}$ ( $\text{M} \cdot \text{h}^{-1}$ ) <sup>-1</sup>	$\overline{k_{w(3c)}}$ ( $\text{h}^{-1}$ )	$\overline{k_{w(4c)}}$ ( $\text{h}^{-1}$ )	$\frac{\overline{k_{w(3c)}}}{\overline{k_{w(1,1)}}}$ (M)	$\frac{\overline{k_{w(4c)}}}{\overline{k_{w(1,1)}}}$ (M)
D	$4.4 \pm 3\%$	$1.9 \pm 4\%$	$0.21 \pm 3\%$	$1.1 \pm 30\%$	$1.3 \pm 23\%$	$4.3 \pm 6\%$	8.8	20
T	$1.4 \pm 3\%$	$0.52 \pm 5\%$	$0.036 \pm 12\%$	‡	‡	$1.4 \pm 12\%$	‡	9.2

\*Figure 3 shows the comparison between calculated concentrations using these rate coefficients and the experimental data. Rate coefficients pertain to water-producing condensation and are defined in the text and in the Appendix.

‡Not measured.

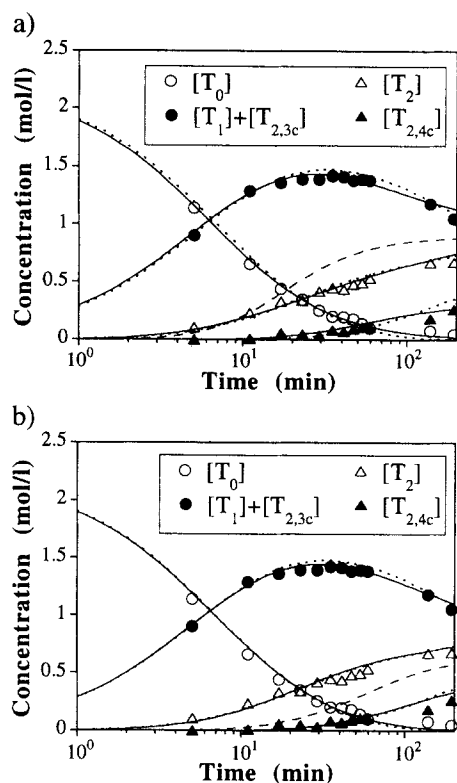


**Figure 4.** Results of fitting the polycondensation model in the Appendix to 7 system NMR data with  $k_{\text{eff}(3c)} = \text{(a) } 6 \text{ h}^{-1} \text{ or (b) } 0.6 \text{ h}^{-1}$ .

Points are experimental data. Solid lines are new fits to these data keeping  $k_{\text{eff}(3c)}$  fixed to the desired value and assuming that points assigned to  $[T_1]$  in Figure 3b are actually  $[T_1] + [T_{2,3c}]$ . Dotted lines represent the fit obtained assuming that  $k_{\text{eff}(3c)} = 0$  (from Figure 3b). Dashed lines are the calculated concentrations of  $T_{2,3c}$  with the new best-fit parameters.

data for polycondensing methylethoxysilanes. This verifies our hypothesis that the mathematical model we have described captures the early-conversion features of methylethoxysilane polycondensation. Now we turn our attention to how well the rate coefficients conform to previously proposed trends that assume that all sites react by the same catalytic mechanism. We know that we must be wary of such an assumption since it has been shown (Pohl and Osterholtz, 1985, 1986; Šefčík and McCormick, 1997a) that the dominant mechanism (acid- or base-catalyzed) depends not only on the pH but also on the degree of siloxane and organic substitution at the reacting sites.

#### Methyl vs. ethyl substitution

Before discussing the effects of methyl and ethyl substitution on condensation reactivity, it is worthwhile to comment on hydrolysis. It is well known that methyl groups accelerate hydrolysis under acidic conditions. This has been observed with alkyl substitution for methylethoxysilanes (Schmidt et al., 1984; Hook, 1996), methylmethoxysilanes (Smith, 1986), and ethylethoxysilanes (Sanchez et al., 1996). However, hydrolysis proceeds too quickly in our samples to measure its kinetics with ordinary  $^{29}\text{Si}$  NMR at room temperature. As mentioned earlier, hydrolysis equilibrium coefficients for methylethoxysi-

lanes vary little with methyl substitution, so observed kinetic differences must be caused by the effects of substitution on the transition-state free energy. In any event, since hydrolysis pseudoequilibrium applies for all of these samples, we can still measure and compare condensation-rate coefficients of different monomers (we discuss copolymerization below).

Figure 5 shows the bimolecular condensation-rate coefficients  $\{\bar{k}_{w(i,i')}\}$  measured for the present methylethoxysilane series, and it also shows the dimerization rate coefficients measured for ethylethoxysilanes (from Sanchez et al., 1996) for comparison. While ethyl addition causes a monotonic decrease in  $k_{00}$ , methyl substitution causes a monotonic increase. Since we enjoy a comparison of rate coefficients for the reaction of single molecules (monomers), we expect that theoretical and empirical models of substituent effects can provide insight into these trends.

Both Lasocki (1964b) and Osterholtz and Pohl (1992) rationalize organosilicon reactivity trends using traditional linear free energy relationship (LFER) arguments, that is, group contributions to reactivity due to both electronic and steric effects (Wells, 1968). They correlate reactivity trends with a modified Taft equation with stronger steric than polar effects. These effects imply that addition of larger and bulkier organic groups decelerates silanediol condensation for steric reasons (Lasocki, 1964b), but that when comparing two molecules with one bulky organic group (say,  $\gamma$ -organopropyl), substitution of OH with Me reduces reactivity slightly, as expected by electronic induction effect arguments (Pohl and Osterholtz, 1986). The acid-catalyzed reaction scheme that emerges consists of a silanol protonation equilibrium (Eq. 5) followed by an  $S_N2$  attack of the protonated site by an unprotonated site (Eq. 6), expelling a protonated water molecule. Steric effects are likely to have an important role in the transition state of the  $S_N2$  step ( $S$  is a solvent molecule):

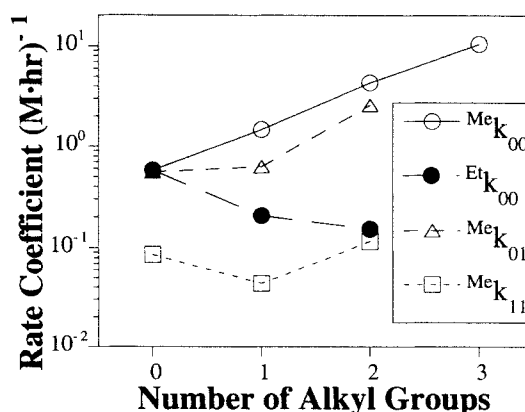
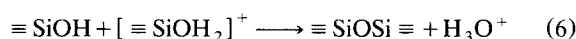


**Figure 5.** Condensation reactivity trends with alkyl substitution.

Trends in all measured rate coefficients of methylethoxysilanes ( $^{\text{Me}}k_{ii'}$ ) with methyl substitution, and trend in ethylethoxysilane dimerization coefficient ( $^{\text{Et}}k_{00}$ ) with ethyl substitution [data from Sanchez et al. (1996)] are plotted as a function of degree of organic substitution (monomers are  $R_x(\text{OEt})_{4-x}\text{Si}$ ).



To explore electronic effects further, we perform semiempirical molecular orbital calculations. Of course, the actual values obtained by these calculations are not yet predictive for silicates, but the trends observed should tell us something about substitution effects. Based on Eq. 6, we take as measures of condensation reactivity the partial charge of the Si nucleus in the protonated species and the partial charge at the Si-OH oxygen of the nucleophile (nonprotonated species). Another measure of reactivity is the ease with which the Si-O bond can be broken in the protonated species, which can be estimated by the Si-OH<sub>2</sub> bond order from the MNDO calculation. As the bond order decreases, the ease of breaking the Si-OH<sub>2</sub> bond increases and so should condensation reactivity.

Table 5 contains the MNDO results for the series of singly hydrolyzed methylethoxysilane and ethylethoxysilane monomers {R<sub>x</sub>(OC<sub>2</sub>H<sub>5</sub>)<sub>3-x</sub>SiOH, R = CH<sub>3</sub>, or C<sub>2</sub>H<sub>5</sub>}. Similar trends are seen (but not shown) for fully hydrolyzed monomers. For both types of alkyl substitution, we observe identical trends. The partial charge at silicon decreases and at OH increases monotonically as ethoxyl groups are replaced with alkyl groups, implying a steady drop in reactivity. The Si-OH<sub>2</sub> bond order drops with the first alkyl substitution, but increases thereafter, also indicating a decrease in reactivity. If these measures are truly indicative of condensation reactivity, then both methyl and ethyl substitution should induce the same changes, most likely negative.

The electronic effects predicted by MNDO calculations are at odds with the experimental observation of opposing reactivity effects of methyl and ethyl substitution of ethoxyl groups. Steric effects can explain this discrepancy. The methyl groups is more compact than either the ethyl or ethoxyl group, so while replacing an ethoxyl with an ethyl group may have little steric effect, replacing an ethoxyl with a methyl group should have a large positive steric effect on condensation reactivity. These ideas are brought together in Table 6: while methyl and ethyl substitution induce similar <sup>29</sup>Si NMR chemical shift changes (indicative of electronic effects) and inductive effects by MNDO, the predominance of steric effects

**Table 6. Summary of <sup>29</sup>Si NMR Chemical Shift, Inductive, Steric, and Condensation Reactivity Trends for Alkylethoxysilanes as Ethoxyl Groups are Substituted\***

Substitution	Δδ( <sup>29</sup> Si)	Inductive Effect	Steric Effect	Condensation React. Effect
(OC <sub>2</sub> H <sub>5</sub> ) → (CH <sub>3</sub> )	Large, +	-	+	+
(OC <sub>2</sub> H <sub>5</sub> ) → (C <sub>2</sub> H <sub>5</sub> )	Large, +	-	sl. +	-
(OC <sub>2</sub> H <sub>5</sub> ) → (OH)	Small, variable	sl. +	sl. +	?(small)
(OC <sub>2</sub> H <sub>5</sub> ) → (OSi)	Moderate, -	+	-	-

\*A plus (+) indicates a positive effect, a minus (-) a negative effect, a question mark (?) an unknown effect, and the modifier (sl.) a slight effect. For chemical shifts, these effects are changes in frequency, while all other indications are strictly qualitative.

gives rise to the observed trends. This explanation is completely consistent with the silanol condensation literature (Lasocki, 1964b; Pohl and Osterholtz, 1986).

The other trends in Figure 5 are consistent with a combination of steric and electronic effects of alkyl substitution. For  $k_{w(0,1)}$ , methyl substitution accelerates condensation, but the effect might be smaller than for  $k_{w(0,0)}$  because one bulky group (siloxane) is already attached to one of the reacting sites. For  $k_{w(1,1)}$ , the first methyl substitution retards condensation, perhaps due to the presence of a bulky siloxane group on both sites. The second methyl addition accelerates condensation, though, perhaps due to a steric effect similar to that observed by Pohl and Osterholtz (1986) for alkylsilanols. A similar interplay of steric and inductive effects was invoked in rationalizing the condensation reactivity trends observed for the series of ethylethoxysilanes hydrolyzed under similar conditions (Sanchez et al., 1996).

### Connectivity effect

The bimolecular condensation rate coefficients reported in Table 4 show that, regardless of the degree of organic substitution of the monomer, condensation is autodecelerating (reactivity decreases as site connectivity increases); this is consistent with previous observations for other alkoxysilanes and organically modified alkoxysilanes (Lasocki, 1963; Pouxviel and Boilot, 1987; Assink and Kay, 1988b; Brunet and Cabane, 1993). However, the substitution effect does not conform to simplified forms proposed in the literature.

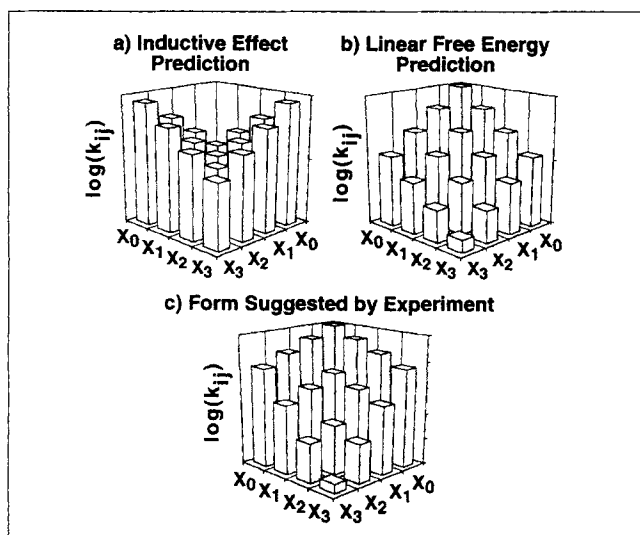
Figure 6a shows one of the rate-coefficient matrix forms proposed on the basis of electronic induction effects. If (1) basicity decreases monotonically as siloxyls replace hydroxyls or alkoxyls, and (2) condensation is fastest between sites differing most in basicity due to differences in the extent of Eq. 5 [as reasonably proposed by Iler (1979)], then one may propose the form  $k_{ii'} \propto C^{|i-i'|}$ , where  $C$  is a constant larger than one. [For very large  $C$ , this form implies that growth would occur mainly by monomer addition to slowly formed nuclei. However, this acidity/basicity argument alone would imply the same trend regardless of pH; this does not agree with the bulk of the data in the literature, which suggests a major pH effect on reactivity and structure (Brinker and Scherer, 1990).] Our findings (Table 4 and Figure 6c), though, do not match this form, perhaps because there are also other effects at play.

Figure 6b shows another form that has been proposed in the literature, based on a LFER. If one assumes that the

**Table 5. MNDO Results: Partial Charges and Bond Orders Indicative of Condensation Reactivity for The Listed Monomers and Dimers\***

Molecule	Partial Charge		Si-OH <sub>2</sub> Bond Order (Protonated)
	@ Si (Protonated)	@ OH (Unprotonated)	
(CH <sub>3</sub> ) <sub>3</sub> SiOH	1.42	-0.626	0.443
(CH <sub>3</sub> ) <sub>2</sub> (C <sub>2</sub> H <sub>5</sub> O)SiOH	1.61	-0.644	0.412
(CH <sub>3</sub> ) <sub>2</sub> (C <sub>2</sub> H <sub>5</sub> O) <sub>2</sub> SiOH	1.75	-0.657	0.407
(C <sub>2</sub> H <sub>5</sub> O) <sub>3</sub> SiOH	1.92	-0.655	0.420
(C <sub>2</sub> H <sub>5</sub> ) <sub>3</sub> SiOH	1.46	-0.627	0.444
(C <sub>2</sub> H <sub>5</sub> ) <sub>2</sub> (C <sub>2</sub> H <sub>5</sub> O)SiOH	1.63	-0.652	0.417
(C <sub>2</sub> H <sub>5</sub> ) <sub>2</sub> (C <sub>2</sub> H <sub>5</sub> O) <sub>2</sub> SiOH	1.76	-0.658	0.403
[(CH <sub>3</sub> ) <sub>2</sub> SiOH] <sub>2</sub> O	1.63	-0.656	0.388
[(CH <sub>3</sub> ) <sub>2</sub> (C <sub>2</sub> H <sub>5</sub> O)SiOH] <sub>2</sub> O	1.78	-0.669	0.398
[(C <sub>2</sub> H <sub>5</sub> O) <sub>2</sub> SiOH] <sub>2</sub> O	1.96	-0.659	0.409
(CH <sub>3</sub> ) <sub>2</sub> Si(OH) <sub>2</sub>	1.58	-0.650	0.411
(CH <sub>3</sub> ) <sub>2</sub> (C <sub>2</sub> H <sub>5</sub> O)Si(OH) <sub>2</sub>	1.72	-0.660	0.404
(C <sub>2</sub> H <sub>5</sub> O) <sub>2</sub> Si(OH) <sub>2</sub>	1.90	-0.652	0.422

\*Calculations were performed for both the unprotonated form (as written, ≡ SiOH) or the form of the molecule with one hydroxyl group protonated ([≡ SiOH<sub>2</sub>]<sup>+</sup>).



**Figure 6. Condensation reactivity trends with connectivity.**

(a) Expected trend based on electronic induction argument:  $k_{ij} = R^{(i-j)}$ . (b) Expected trend with a linear free-energy relationship:  $k_{ij} = R^{(i+j)}$ . (c) A function similar to the experimentally observed trend:  $k_{ij} = R_1^{\min(i,j)} R_2^{\max(i,j)}$ .

activation energy for condensation is given by the sum of constant contributions for each group attached to the reacting sites (discounting the effects of hydrolysis degree), the predicted form is  $k_{ii'} \propto k_i k_{i'}$  where  $\{k_i\}$  are constant. Ling (1992) reported some success applying this model to tetraethoxysilane polycondensation. If the change in activation free energy for each siloxyl substitution at either site is assumed to be constant, we arrive at the form proposed by Brinker and Assink (1989):  $k_{ii'} \propto R^{(i+i')}$ . This form allows for either autoacceleration ( $R > 1$ ) or autodeceleration ( $R < 1$ ). An example of the shape predicted is shown in Figure 6b. An attractive feature of these LFERs is that they permit relatively easy structural modeling for nonlinear polycondensation (Sarmoria and Miller, 1991). Unfortunately, our findings (Table 4 and Figure 6c) do not match either form of LFER.

The experimentally determined bimolecular rate coefficient drops only mildly as the connectivity of *one* of the pair of reacting sites increases ( $k_{00}$ , cf.  $k_{01}$ ). However, it drops sharply when the connectivity of *both* sites increases ( $k_{00}$ , cf.  $k_{11}$ ). In contrast to the prediction of LFER matrices,  $(k_{11}/k_{00}) \neq (k_{01}/k_{00})^2$ . Substitution effects similar to the pattern in Figure 6c have also been reported for tetraethoxysilane and ethylethoxysilanes (Sanchez et al., 1996) and for methyltrimethoxysilane (Smith, 1987).

The simplest function consistent with the experimental trend is  $k_{ii'} \propto R_1^{\min(i,i')} R_2^{\max(i,i')}$ , where  $R_1$  and  $R_2$  are constants with  $R_1 < R_2$ . Figure 6c is an example of this rate coefficient matrix for  $R_1 = 0.07$  and  $R_2 = 0.4$ . The matrix is a tiered structure. It is neither a valley (Figure 6a), nor a ridge (as in Figure 6a with  $C < 1$ ), nor a mountain (Figure 6b), nor a sinkhole (as in Figure 6b with  $R > 1$ ). The data in Table 4 are consistent with  $(R_1, R_2)$  being (0.11, 0.43) for  $D$  and (0.07, 0.35) for  $T$ —far from the case proposed by Brinker and Assink (1989) ( $R_1 = R_2$ ) for acid-catalyzed tetraethoxysilane polymerization. One might be tempted to flatten the tiers of

the rate-coefficient matrix, for example, taking  $R_2$  to be 1 and fitting only  $R_1$  to the data. As one might guess from the values found for  $D$  and  $T$ , however, doing this allows only a poor fit.

To understand the effects of siloxyl substitution, we return to the mechanism for acid-catalyzed silanol condensation in Eqs. 5 and 6 (Osterholtz and Pohl, 1992). If we accept this mechanism, we can use MNDO calculations to examine dimers and, by comparing them to monomers to get some idea of what inductive effects to expect. Table 5 shows that partial charges do not change much as a result of substituting siloxyl groups for ethoxyl groups, but that the order of the Si-OH<sub>2</sub> bond does decrease as a result of the substitution, implying a greater condensation reactivity for reasons discussed in the previous section. This contradicts the experimental observation (siloxyl substitution slows condensation), so we conclude that the observed effect is more consistent with a steric effect on the substitution stage of the condensation reaction (Eq. 6).

Table 6 summarizes these conclusions: we observe a moderate change in <sup>29</sup>Si chemical shift with siloxyl substitution and we expect a positive electronic inductive effect from the MNDO calculations, but the observed effect is negative, so there must be a negative steric effect on condensation reactivity. The reactivity decrease is small when the connectivity of only one of the reacting pairs increases because the reaction can still proceed at the less-connected site. When the connectivity of both sites increases, though, the reaction must proceed at a more connected site and the reactivity decreases substantially.

### Hydrolysis effect on condensation reactivity

On a conversion scale, identical lumped site distributions  $\{T_i\}$  to those we measured have been reported under quite different conditions for methyl-substituted trifunctional monomer polycondensation: by Liu and Kim (1996) in a methanol/ethanol/water mixture with  $[HCl] = 0.1$  M and limited water, and by Devreux et al. (1990) at pH 2 in ethanol with excess water. This implies that the substitution effect is insensitive to small changes in pH and water concentration (and hence to degrees of hydrolysis) [because different sites have different isoelectric points, their pH dependence may be such that the substitution effect *will* change with pH at some point in the range 2 to 6 (as discussed by Šefčík and McCormick (1997a))].

Table 6 also includes a row for the effect of hydrolysis. The effect of substituting an ethoxyl with a hydroxyl is actually difficult to assess. We know first of all that the <sup>29</sup>Si NMR chemical-shift change is relatively small and that, in fact, its direction depends on the functionality of the site (another indication that it is subtle). If the chemical shift is correlated to an inductive effect (Rühlmann et al., 1995), we expect it to be small. MNDO calculations (Table 5) comparing doubly and singly hydrolyzed monomers indicate that ethoxyl-to-hydroxyl substitution results in a slight decrease in the partial charge at silicon in the protonated form, a slight decrease in the partial charge at oxygen in the unprotonated form, and a slight reduction in bond order. The first effect indicates a decrease in reactivity, but the latter two effects indicate an increase. Thus, we cannot speculate on the direction of the induced

effect except to say that it should be small [the picture from organic chemistry is that this effect should be positive (Brinker and Scherer, 1990)]. Since the OH group is somewhat smaller in van der Waals radius than the OEt group, we may also guess that there should be slight positive steric effect, but we see no evidence for a strong substitution effect of hydroxyl groups on condensation reactivity from the experiments carried out here. The only real way to check for this is to vary the water content, in which case the effects of alcohol-producing condensation and activity coefficient variations must be considered. We are investigating this further.

### Cyclization

We observe substantial formation of four-silicon rings in the *D* and *T* systems (cyclization is of course impossible for *M*). Using the rate coefficients reported in Table 4, we can characterize the tendency for cyclization by considering  $\bar{k}_{w(4c)}/\bar{k}_{w(1,1)}$ . This ratio, which has units of concentration, represents (in a sense) the effective concentration of attached chain ends as seen by the site at the other end of a linear tetramer [see Stepto (1981) for an insightful discussion of this concept]. It is greater for *D* than for *T*, and greater for *T* than for *Q* (Ng and McCormick, 1996). Evidently methyl groups encourage four-silicon ring formation. All values are high enough, though, that it is absolutely necessary (given the molar volumes of the pure tetramers) to include unimolecular cyclization to find meaningful rate constants and to construct a meaningful mathematical model of this process.

The kinetic favorability and stability of four-silicon rings contribute to the difficulty of preparing homogeneous polydimethylsiloxane(PDMS)-silica hybrid materials. For instance, Hoshino and Mackenzie (1995) report that when a low molecular weight PDMS oligomer is reacted with *Q* monomers, an equilibrium concentration of cyclic tetramers persists. While these tetramers could serve as a renewable source of four-membered PDMS chains, they could also represent a significant fraction of Si-O-Si bonds that do not contribute to network formation. It may be best to reduce their concentration by, for instance, introducing monomer or trimers steadily to avoid a large concentration of tetramers. The implications of these strong cyclization reactions for network growth in sol-gel materials are addressed by Kasehagen et al. (1997).

For the *Q* system, three-silicon rings form at a reasonable rate:  $\bar{k}_{w(3c)}/\bar{k}_{w(1,1)} = 2.1$  at pH 3.3 (Sanchez and McCormick, 1994). For the *T* system, we could not determine this ratio, but the value could easily be of this order of magnitude. For the methyl-*D* system, three-silicon rings are even more kinetically favorable ( $\bar{k}_{w(3c)}/\bar{k}_{w(1,1)} = 6.0$ ), but they appear to be thermodynamically unstable. The concentration of these rings rises and then falls again before a significant concentration builds up (Figure 3a). Since the rings cannot condense further, ring opening is the only way to explain the shape of this curve. For the ethyl-*D* system, on the other hand, three-silicon rings form quickly and accumulate in the  $^{29}\text{Si}$  NMR spectra (Sanchez et al., 1996), indicating either greater stability of  $[(\text{Et})_2\text{SiO}]_3$  than  $[(\text{Me})_2\text{SiO}]_3$  or merely a smaller net siloxane hydrolysis rate.

In a separate article, we will discuss in detail the inaccuracies associated with the use of models without cyclization.

When cyclization is included, the substitution effect proves to be more severe than the model without cyclization predicts (Ng and McCormick, 1996). Strong cyclization combined with a severe negative substitution effect is consistent with a sharp initial conversion rise followed by a sudden change to a gradual conversion increase as gelation is approached in TEOS systems and may result in preliminary formation of a distribution of compact, cagelike species (Ng et al., 1995).

### Implication for copolymerization

The trends observed with alkyl substitution allow us to comment on strategies that might be needed to promote a homogeneous site distribution in copolymers derived from alkylethoxysilanes. The most common strategy is "prehydrolysis," in which the monomer thought to be less reactive (in what sense is not always clear) is allowed to react with water for some time before adding the other monomer(s).

Since hydrolysis equilibrium coefficients are similar for the ethoxysilanes studied [and for other systems (Rankin et al., 1998b)], copolymerizing monomers should have hydroxyls randomly distributed among uncondensed groups at pseudoequilibrium. In cases where hydrolysis does reach pseudoequilibrium, copolymer structure development is dictated strictly by condensation kinetics, so we can consider primarily condensation trends in suggesting copolymerization strategies. We have shown that hydrolysis reaches pseudoequilibrium during MD copolymerization (Rankin et al., 1997), as have Prabakar and Assink (1997) for a *TQ* system. On the other hand, this condition should be violated when the kinetics of hydrolysis and reesterification differ so much that one monomer approaches hydrolysis pseudoequilibrium significantly before the other. Sugahara and coworkers have demonstrated significantly differing hydrolysis time scales for *T* and *Q* monomers during copolymerization under a different set of conditions (Sugahara et al., 1992b). For *TQ* copolymerization under HCl and water concentrations identical to this work, we have also observed a transient during which the *T* monomer reaches pseudoequilibrium and *Q* hydrolyzes more slowly.

Methyl substitution produces similar trends in both hydrolysis and condensation, so the rates of both reactions can be controlled simultaneously. The simplest strategy would be to allow the less methyl-substituted monomer to hydrolyze for some time before adding a more methyl-substituted monomer. Because methyl substitution accelerates *both* hydrolysis and condensation, some time frame can be found where the less methyl-substituted is hydrolyzed without too much condensation, and hydrolysis and condensation of the more methyl-substituted monomer will "catch up" quickly once it is added.

However, because of differences in the effect of connectivity on condensation reactivity, this two-stage scheme may not provide optimal homogeneity. Another strategy is to use less of the more methyl-substituted component to reduce homcondensation of that component. This has been shown to provide materials with a homogeneous distribution of methyl groups in *TQ* and *DQ* gels, but the compositions for which this is possible are limited (De Witte et al., 1996). A more general strategy with more potential for homogeneity is to use a semibatch reactor configuration in which all of the less-reactive component is present throughout and the

more-reactive component is added continuously. The time program of addition of the more-reactive monomer can be controlled to maximize homogeneity.

For ethyl substitution, on the other hand, allowing the less ethyl-substituted monomer to react on its own before adding the more ethyl-substituted monomer will promote its hydrolysis, but its condensation may be too slow for it to be well-incorporated with the other component. Since even larger organic groups are expected to induce reduced condensation reactivity as well (Lasocki, 1963), we expect that a two-stage semibatch process (where the less-substituted monomer is prehydrolyzed) may not be sufficient to promote homogeneity with these monomers. This could explain the reported difficulty in promoting homogeneity by prehydrolysis for copolymers from tetraethoxysilane and a triethoxysilane with a bulky organic group (Kim et al., 1993). If hydrolysis is very fast for both monomers, a semibatch reactor with the more-alkyl-substituted monomer present throughout (i.e., the opposite of the recommendation for methyl-substituted monomers) should be used.

Given the differing autodeceleration trends for different monomers, and given the possibility of cyclization, these recommendations for controlling copolymer homogeneity need further development. As more detailed polymerization models evolve for these systems, it will become possible to explore and optimize more complex reactor schemes. These may include time-programmed semibatch reactors and combinations of continuous reactors of interest not only for optimizing homogeneity but also for commercialization. Some combinations of monomers may require a series of reactors to promote homogeneity in the copolymer product.

## Conclusions

The principal results reported here are the complex substitution effects in the condensation rate coefficients of methylthoxysilanes. To determine them, we have proposed and applied a new kinetic polymerization model. This model includes features to account for hydrolysis pseudoequilibrium, first shell substitution effects, and (limited) cyclization. The model robustly matches experimental data at early conversions.

We find similar hydrolysis equilibrium coefficients regardless of the degree or type of organic substitution on the monomer. This implies that in a binary copolymer system, if hydrolysis pseudoequilibrium of both monomers is reached, then condensation kinetics alone govern copolymer homogeneity.

We observe a strikingly different trend for methyl group substitution of ethoxyl groups than that for ethyl substitution. Whereas ethyl addition to ethoxysilane monomers retards dimerization, methyl addition accelerates it. This effect may be consistent with a combination of strong steric effects and weak inductive effects governing condensation reactivity.

We observe similar autodecelerating polycondensation trends for all monomers. The form of the first shell substitution effect is similar to that observed previously for ethylethoxysilanes (Sanchez et al., 1996) and does not conform to a simple form such as that suggested by a linear free energy relationship.

All systems favor four-silicon ring formation under the conditions used: tetraethoxysilane least, then methyltri-

ethoxysilane, and dimethyldiethoxysilane most. Three-silicon rings are not detected for trifunctional systems, but they are formed at appreciable rates in the difunctional systems. However, whereas high concentrations of the three-silicon ring accumulate during diethyldiethoxysilane polymerization, we have shown that the ring hydrolyzes and disappears during dimethyldiethoxysilane polymerization.

In terms of copolymerization, the differences in trends observed for ethyl and methyl substitution indicate that (1) non-simple reactor schemes will typically be necessary to promote homogeneity, and (2) different organic groups may call for quite different copolymerization strategies.

## Acknowledgments

We gratefully acknowledge a fellowship to S.E.R. from the National Science Foundation, research support from Dow Corning Corporation, and use of the facilities of the Center for Interfacial Engineering and the Minnesota Supercomputer Institute at the University of Minnesota. We also thank Dr. Ján Šefčík of California Institute of Technology, Dr. Leo Kasehagen of Elf Atochem, and Dr. Gary Wieber and Dr. Randall Schmidt of Dow Corning Corporation for helpful discussions.

## Literature Cited

- Alam, T. M., R. A. Assink, and D. A. Loy, "Hydrolysis and Esterification in Organically Modified Alkoxysilanes: A  $^{29}\text{Si}$  NMR Investigation of Methyltrimethoxysilane," *Chem. Mater.*, **8**, 2366 (1996a).  
Alam, T. M., R. A. Assink, S. Prabakar, and D. A. Loy, "Identification and Characterization of the Hydrolysis Products in TMOS and MTMS Monomers using  $^{29}\text{Si}$  NMR and Polarization Transfer Techniques," *Magn. Reson. Chem.*, **34**, 603 (1996b).  
Assink, R. A., and B. D. Kay, "Sol-Gel Kinetics I. Functional Group Kinetics," *J. Non-Cryst. Sol.*, **99**, 359 (1988a).  
Assink, R. A., and B. D. Kay, "Sol-Gel Kinetics III. Test of the Statistical Reaction Model," *J. Non-Cryst. Solids*, **107**, 35 (1988b).  
Assink, R. A., and B. D. Kay, "The Chemical Kinetics of Silicate Sol-Gels: Functional Groups Kinetics of Tetraethoxysilane," *Colloids Surf. A*, **74**, 1 (1993).  
Bailey, J. K., C. W. Macosko, and M. L. Mecartney, "Modeling the Gelation of Silicon Alkoxides," *J. Non-Cryst. Solids*, **125**, 208 (1990).  
Baney, R. H., M. Itoh, A. Sakakibara, and T. Suzuki, "Silsequioxanes," *Chem. Rev.*, **95**, 1409 (1995).  
Barry, A. J., and H. N. Beck, "Silicone Polymers," *Inorganic Polymers*, F. G. A. Stone and W. A. G. Graham, eds., Academic Press, New York (1962).  
Brinker, C. J., and R. A. Assink, "Spinnability of Silica Sols. Structural and Rheological Criteria," *J. Non-Cryst. Solids*, **111**, 48 (1989).  
Brinker, C. J., and G. W. Scherer, *Sol-Gel Science: The Physics and Chemistry of Sol-Gel Processing*, Academic Press, Boston (1990).  
Brunet, F., and B. Cabane, "Populations of Oligomers in Sol-Gel Condensation," *J. Non-Cryst. Solids*, **163**, 211 (1993).  
Brus, J., J. Karhan, and P. Kotlík, " $^{29}\text{Si}$  NMR Study of Distribution of Oligomers in Polycondensation of Tetraethoxysilane," *Collect. Czech. Chem. Commun.*, **61**, 691 (1996).  
Brus, J., and P. Kotlík, "Polyacrylate Effects on Tetraethoxysilane Polycondensation," *Chem. Mater.*, **8**, 2739 (1996).  
Cardenas, A., N. Hovnanian, and M. Smaili, "Sol-Gel Formation of Heteropolysiloxanes from Diethylphosphatoethyltriethoxysilane and Tetraethoxysilane," *J. Appl. Polym. Sci.*, **60**, 2279 (1996).  
Chambers, R. C., J. W. E. Jones, Y. Haruvy, S. E. Webber, and M. A. Fox, "Influence of Steric Effects on the Kinetics of Ethyltrimethoxysilane Hydrolysis in a Fast Sol-Gel System," *Chem. Mater.*, **5**, 1481 (1993).  
Chojnowski, J., M. Cypryk, K. Kaźmierski, and K. Różga, "The Reactivity of Monomeric Silanol Intermediates in the Hydrolysis Polycondensation of Tetraethoxysilane in Acidic Media," *J. Non-Cryst. Solids*, **125**, 40 (1990).  
Chojnowski, J., M. Scibiorek, and J. Kowalski, "Mechanism of the Formation of Macrocycles During the Cationic Polymerization of

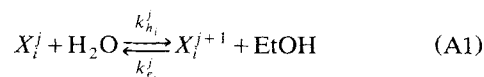
- Cyclotrisiloxanes. End to End Ring Closure Versus Ring Expansion," *Makromol. Chem.*, **178**, 1351 (1977).
- Cihlar, J., "Hydrolysis and Polycondensation of Ethyl Silicates. I. Effect of pH and Catalyst on the Hydrolysis and Polycondensation of Tetraethoxysilane," *Coll. Surf. A*, **70**, 239 (1993).
- Clark, T., *A Handbook of Computational Chemistry*, Wiley, New York (1985).
- Clarson, S. J., and J. A. Semlyen, *Siloxane Polymers*, Prentice Hall, Englewood Cliffs, NJ (1993).
- DeLattre, L., and F. Babonneau, "Influence of the Nature of the R Group on the Hydrolysis and Condensation Process of Trifunctional Silicon Alkoxides, R-Si(OR')<sub>3</sub>," *Better Ceramics Through Chemistry VI*, A. K. Cheetham, C. J. Brinker, M. L. McCartney, and C. Sanchez, eds., Materials Research Society, Pittsburgh, p. 365 (1994).
- DeLattre, L., M. Roy, and F. Babonneau, "Design of Homogeneous Hybrid Materials Through a Careful Control of the Synthetic Procedure," *J. Sol-Gel Sci. Technol.*, **8**, 567 (1997).
- Devreux, F., J. P. Boilot, and F. Chaput, "Sol-Gel Condensation of Rapidly Hydrolyzed Silicon Alkoxides: A Joint <sup>29</sup>Si NMR and Small-Angle X-Ray Scattering Study," *Phys. Rev. A*, **41**, 6901 (1990).
- De Witte, B. M., D. Commers, and J. B. Uytterhoeven, "Distribution of Organic Groups in Silica Gels Prepared from Organo-Alkoxysilanes," *J. Non-Cryst. Solids*, **202**, 35 (1996).
- Dotson, N. A., R. Galván, R. L. Laurence, and M. Tirrell, *Polymerization Process Modeling*, VCH, New York (1996).
- Doughty, D. H., R. A. Assink, and B. D. Kay, "Hydrolysis and Condensation Kinetics of Dimeric Sol-Gel Species by <sup>29</sup>Si NMR Spectroscopy," *Silicon-Based Polymer Science: A Comprehensive Resource*, J. M. Zeigler, and F. W. G. Feuron, eds., ACS, Washington, DC, p. 241 (1990).
- Fyfe, C. A., and P. P. Aroca, "Quantitative Kinetic Analysis by High-Resolution <sup>29</sup>Si NMR Spectroscopy of the Initial Stages in the Sol-Gel Formation of Silica Gel from Tetraethoxysilane," *Chem. Mater.*, **7**, 1800 (1995).
- Gordon, M., and W. B. Temple, "The Graph-Like State of Molecules III. Ring-Chain Competition Kinetics in Linear Polymerisation Reactions," *Makromol. Chem.*, **160**, 263 (1972).
- Grubb, W. T., "A Rate Study of the Silanol Condensation Reaction at 25° in Alcoholic Solvents," *J. Amer. Chem. Soc.*, **76**, 3408 (1954).
- Guibergia-Pierron, M., and G. Sauvet, "Heterofunctional Condensation of Alkoxysilanes and Silanols—I. Synthesis of Definite Polysiloxane Networks," *Eur. Polym. J.*, **28**, 29 (1992).
- Harris, R. K., *Nuclear Magnetic Resonance Spectroscopy. A Physico-Chemical View*, Wiley, New York (1986).
- Harris, R. K., and M. L. Robins, "<sup>29</sup>Si Nuclear Magnetic Resonance Studies of Oligomeric and Polymeric Siloxanes: 4. Chemical Shift Effects of End-Groups," *Polymer*, **19**, 1123 (1978).
- Helary, G., and G. Sauvet, "Heterofunctional Condensation of Alkoxysilanes and Silanols—II. Synthesis of Linear Poly(aminoalkylsiloxane)s," *Eur. Polym. J.*, **28**, 37 (1992).
- Hook, R. J., "A <sup>29</sup>Si NMR Study of the Sol-Gel Polymerisation Rates of Substituted Ethoxysilanes," *J. Non-Cryst. Solids*, **195**, 1 (1996).
- Hoshino, Y., and J. D. Mackenzie, "Viscosity and Structure of Ormosil Solutions," *J. Sol-Gel Sci. Technol.*, **5**, 83 (1995).
- Iler, R. K., *The Chemistry of Silica*, Wiley, New York (1979).
- Kasehagen, L. J., S. E. Rankin, A. V. McCormick, and C. W. Macosko, "Modeling FSSE and Preferred Cyclization in Sol-Gel Polymerization," *Macromol.*, **30**, 3921 (1997).
- Kazmierski, K., J. Chojnowski, and J. McVie, "The Acid-Catalyzed Condensation of Methyl Substituted Model Oligosiloxanes Bearing Silanol and Ethoxysilane Functions," *Eur. Polym. J.*, **30**, 515 (1994).
- Kelling, H., K. Lange, and A. Surkus, "On the Acid-Catalyzed Reaction of Siloxanes with Alcohols," *Organosilicon Chemistry. From Molecules to Materials*, N. Aubert and J. Weis eds., VCH, Weinheim, p. 67 (1994).
- Kelts, L. W., and N. J. Armstrong, "A Silicon-29 NMR Study of the Structural Intermediates in low pH Sol-Gel Reactions," *J. Mater. Res.*, **4**, 423 (1989).
- Kim, J., J. L. Plawsky, E. Van Wagenen, and G. M. Korenowski, "Effect of Processing Parameters and Polymerization Behavior on the Nonlinear Optical Response of Sol-Gel Materials," *Chem. Mater.*, **5**, 1118 (1993).
- Klemperer, W. G., and S. D. Ramamurthi, "A Flory-Stockmayer Analysis of Silica Sol-Gel Polymerization," *J. Non-Cryst. Solids*, **121**, 16 (1990).
- Kumar, A., and S. Misra, "A Kinetic Approach to Multifunctional Polymerization with Cyclization," *Poly. Sci. Eng.*, **26**, 1297 (1986).
- Lasocki, Z., "Substitution at a Silicon Atom in Organosilicon Compounds: I. Rates of Condensation of Straight-Chain Alkyl Substituted Silanediols," *Bull. Acad. Polon. Sci., Sér. Sci. Chim.*, **11**, 637 (1963).
- Lasocki, Z., "Substitution at a Silicon Atom in Organosilicon Compounds: II. Rates of Condensation of Branched-Chain Alkyl-Substituted Silanediols," *Bull. Acad. Polon. Sci., Sér. Sci. Chim.*, **12**, 223 (1964a).
- Lasocki, Z., "Substitution at a Silicon Atom in Organosilicon Compounds: III. Steric and Polar Effects of Alkyl Groups in the Condensation of Silanediols," *Bull. Acad. Polon. Sci., Sér. Sci. Chim.*, **12**, 227 (1964b).
- Ling, D. A., "Primary Structural Evolution in Acid-Catalyzed Silica Polysol-Gel Processes," PhD Thesis, Georgia Institute of Technology, Atlanta (1992).
- Liu, J., and S. D. Kim, "Polycondensation Behavior of Methyltrimethoxysilane Studied by NMR Spectroscopy," *J. Poly. Sci. B: Polym. Phys.*, **34**, 131 (1996).
- Lux, P., F. Brunet, J. Virlet, and B. Cabane, "Combined DEPT 1D and INEPT DQF COSY 2D Experiments in <sup>29</sup>Si NMR Spectroscopy of Alkoxysilane Polymers 2," *Magn. Reson. Chem.*, **34**, 173 (1996).
- Maas, U., and S. B. Pope, "Simplifying Chemical Kinetics: Intrinsic Low-Dimensional Manifolds in Composition Space," *Combust. Flame*, **88**, 239 (1992).
- Mark, J. E., C. Y.-C. Lee, and P. A. Bianconi, eds., *Hybrid Inorganic-Organic Composites*, ACS Symp. Ser., Vol. 585, American Chemical Society, Washington, DC (1995).
- Marsmann, H., "<sup>29</sup>Si-NMR Spectroscopic Results," *NMR: Basic Principles and Progress*, P. Diehl, E. Fluck, H. Gunther, R. Dosfeld, and J. Seelig, eds., Springer-Verlag, Berlin, p. 65 (1981).
- Ng, L. V., and A. V. McCormick, "Acidic Sol-Gel Polymerization of TEOS: Effect of Solution Composition on Cyclization and Bimolecular Condensation Rates," *J. Phys. Chem.*, **100**, 12517 (1996).
- Ng, L. V., P. Thompson, J. Sanchez, C. W. Macosko, and A. V. McCormick, "Formation of Cage-like Intermediates from Nonrandom Cyclization During Acid-Catalyzed Sol-Gel Polymerization of Tetraethyl Orthosilicate," *Macromol.*, **28**, 6471 (1995).
- Osterholtz, F. D., and E. R. Pohl, "Kinetics of the Hydrolysis and Condensation of Organofunctional Alkoxysilanes: A Review," *Silanes and Other Coupling Agents*, K. L. Mittal, ed., VSP, Utrecht, The Netherlands, p. 119 (1992).
- Peppas, N. A., A. B. Scranton, A. H. Tsou, and D. E. Edwards, "Branching Theory in Sol-Gel Processing," *Better Ceramics Through Chemistry III*, C. J. Brinker, D. E. Clark, and D. R. Ulrich, eds., Materials Research Society, Pittsburgh, p. 43 (1988).
- Pohl, E. R., and F. D. Osterholtz, "Kinetics and Mechanism of Aqueous Hydrolysis and Condensation of Alkyltrialkoxysilanes," *Molecular Characterization of Composite Interfaces*, H. Ishida and G. Kumar, eds., Plenum, New York, p. 157 (1985).
- Pohl, E. R., and F. D. Osterholtz, "Kinetics and Mechanism of Condensation of Alkylsilanols in Aqueous Solution," *Silanes, Surfaces, and Interfaces*, D. E. Leyden, eds., Gordon & Breach, New York, p. 481 (1986).
- Pouxviel, J. C., and J. P. Boilot, "Kinetic Simulations and Mechanisms of the Sol-Gel Polymerization," *J. Non-Cryst. Solids*, **94**, 374 (1987).
- Pouxviel, J. C., J. P. Boilot, J. C. Beloeil, and J. Y. Lallemand, "NMR Study of the Sol/Gel Polymerization," *J. Non-Cryst. Solids*, **89**, 345 (1987).
- Prabakar, S., and R. A. Assink, "Hydrolysis and Condensation Kinetics of Two Component Organically Modified Silica Sols," *J. Non-Cryst. Solids*, **211**, 39 (1997).
- Rankin, S. E., C. W. Macosko, and A. V. McCormick, "Sol-Gel Kinetics for the Preparation of Inorganic/Organic Siloxane Copolymers," *Better Ceramics Through Chemistry VII*, B. K. Coltrain, C. Sanchez, D. W. Schaefer and G. L. Wilkes, eds., Materials Research Society, Pittsburgh, p. 113 (1996).
- Rankin, S. E., C. W. Macosko, and A. V. McCormick, "Copolymerization Kinetics of a Model Siloxane System," *J. Poly. Sci. A*, **35**, 1293 (1997).

- Rankin, S. E., C. W. Macosko, and A. V. McCormick, "Difficulties in Identifying Rate Parameters for Sol-Gel Modeling: Sensitivities and Experimental Signatures," (1998a).
- Rankin, S. E., J. Šefčík, and A. C. McCormick, "Sol-Gel Thermodynamics: II. Similarities in the Hydrolysis Pseudoequilibrium Behavior of Multifunctional Ethoxysilane Systems," (1998b).
- Re, N., "Kinetics of Bicomponent Sol-Gel Processes," *J. Non-Cryst. Solids*, **142**, 1 (1992).
- Rolando, R. J., and C. W. Macosko, "Ring Formation in Linear Stepwise Polymerization," *Macromol.*, **20**, 2707 (1987).
- Rühlmann, K., U. Scheim, and K. Käßler, "Substituent Constants for Groups at the Si-Atom," *Progress in Organosilicon Chemistry*, B. Marciniec and J. Chojnowski, eds., Gordon & Breach, Basel, Switzerland, p. 147 (1995).
- Sanchez, J., and A. McCormick, "Kinetic and Thermodynamic Study of the Hydrolysis of Silicon Alkoxides in Acidic Alcohol Solutions," *J. Phys. Chem.*, **96**, 8973 (1992a).
- Sanchez, J., and A. McCormick, "Kinetics and Equilibrium of Acid-Catalyzed Tetraethoxysilane Hydrolysis," *Chemical Processing of Advanced Materials*, L. L. Hench and J. K. West, eds., Wiley, New York, p. 43 (1992b).
- Sanchez, J., and A. V. McCormick, "Intramolecular vs. Intermolecular Condensation Rates in the Acidic Polymerization of Octaethoxytrisiloxane," *J. Non-Cryst. Solids*, **167**, 289 (1994).
- Sanchez, J., S. E. Rankin, and A. V. McCormick, "<sup>29</sup>Si NMR Kinetic Study of Tetraethoxysilane and Ethyl-Substituted Ethoxysilane Polymerization in Acidic Conditions," *Ind. Eng. Chem. Res.*, **34**, 117 (1996).
- Sarmoria, C., and D. R. Miller, "Models for the First Shell Substitution Effect in Stepwise Polymerization," *Macromol.*, **24**, 1833 (1991).
- Sarmoria, C., E. M. Vallés, and D. R. Miller, "Validity of Some Approximation Used to Model Intramolecular Reaction in Irreversible Polymerization," *Macromol.*, **23**, 580 (1990).
- Schaefer, D. W., G. L. Wilkes, C. Sanchez, and B. Coltrain, eds., *Better Ceramics through Chemistry VII*, Mat. Res. Soc. Symp. Proc., Materials Research Society, Pittsburgh (1996).
- Schmidt, H., H. Scholze, and A. Kaiser, "Principles of Hydrolysis and Condensation Reaction of Alkoxysilanes," *J. Non-Cryst. Solids*, **63**, 1 (1984).
- Šefčík, J., and A. V. McCormick, "Kinetic and Thermodynamic Issues in Sol-Gel Processes Using Silicon Alkoxides," *Catal. Today*, **35**, 205 (1997a).
- Šefčík, J., and A. V. McCormick, "Thermochemistry of Aqueous Silicate Solution Precursors to Ceramics," *AIChE J.*, **43**, 2773 (1997b).
- Šefčík, J., S. E. Rankin, S. J. Kirchner, and A. V. McCormick, "Silanol Esterification, Condensation, and Deprotonation Equilibria," (1998).
- Smith, K. A., "A Study of the Hydrolysis of Methoxysilanes in a Two-Phase System," *J. Org. Chem.*, **51**, 3827 (1986).
- Smith, K. A., "Polycondensation of Methyltrimethoxysilane," *Macromol.*, **20**, 2514 (1987).
- Stanford, J. L., R. F. T. Stepto, and D. R. Waywell, "Rate Theory of Irreversible Linear Random Polymerisation: 2. Application to Intramolecular Reaction in A-A+B-B Type Polymerisations," *J. Chem. Soc. Farad. Trans. I*, **71**, 1308 (1975).
- Stepto, R. F. T., "Intra-Molecular Reaction and Gelation in Condensation or Random Polymerisation," *Network Formation and Cyclisation in Polymer Reactions*, R. N. Haward, ed., Applied Science Publishers, London, p. 81 (1981).
- Stewart, J. J. P., "MOPAC: A Semiempirical Molecular Orbital Program," *J. Comput. Aided Mol. Des.*, **4**, 1 (1990).
- Sugahara, Y., S. Okada, K. Kuroda, and C. Kato, "<sup>29</sup>Si-NMR Study of Hydrolysis and Initial Polycondensation Processes of Organoalkoxysilanes. I. Dimethyldiethoxysilane," *J. Non-Cryst. Solids*, **139**, 25 (1992a).
- Sugahara, Y., S. Okada, S. Sato, K. Kuroda, and C. Kato, "<sup>29</sup>Si-NMR Study of Hydrolysis and Initial Polycondensation Processes of Organoalkoxysilanes. II. Methyltriethoxysilanes," *J. Non-Cryst. Solids*, **167**, 21 (1994).
- Sugahara, Y., Y. Tanaka, S. Sato, K. Kuroda, and C. Kato, "Silicon-29 NMR Study on the Initial Stage of the Coadhydrolysis of Tetraethoxysilane and Methyltriethoxysilane," *Mater. Res. Soc. Symp. Proc.*, **271**, 231 (1992b).
- Tang, A., R. Xu, S. Li, and Y. An, "Characterisation of Polymeric Reaction in Silicic Acid Solution: Intramolecular Cyclization," *J. Mater. Chem.*, **3**, 893 (1993).
- Vainrub, A., F. Devreux, J. P. Boilot, F. Chaput, and M. Sarkar, "Sol-Gel Polymerization in Alkoxysilanes: <sup>29</sup>Si NMR Study and Simulation of Chemical Kinetics," *Mater. Sci. Eng. B.*, **37**, 197 (1996).
- Voronkov, M. G., "Energy of the Si-O Bond and Ring Strain in Permethylcyclotrioxanes," *Russ. J. Gen. Chem.*, **66**, 165 (1996).
- Wells, P. R., *Linear Free Energy Relationship*, Academic Press, London (1968).
- Wilcock, D. F., "Liquid Methylpolysiloxane Systems," *J. Amer. Chem. Soc.*, **69**, 477 (1947).
- Wood, D. L., and E. M. Rabinovich, "Heat Evolution, Light Scattering, and Infrared Spectroscopy in the Formation of Silica Gels from Alkoxides," *J. Non-Cryst. Solids*, **107**, 199 (1989).
- Zhang, Z., Y. Tanigami, and R. Terai, "Preparation of Transparent Methyl-Modified Silica Gel," *J. Non-Cryst. Solids*, **189**, 212 (1995).

## Appendix: Detailed Reactions and Equations

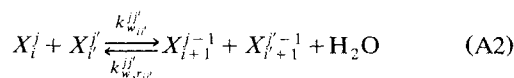
For the sake of brevity and clarity, only a qualitative picture of the condensation reaction scheme was presented in the body of this article. Here, the full set of reactions required are considered and the full set of equations is presented in its most general form. First, we consider the six types of possible reactions occurring at a given site:

Hydrolysis/Reesterification:



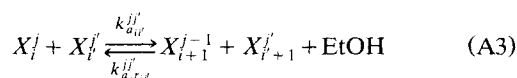
$$i \in [0, f-1]; \quad j \in [0, f-i-1].$$

Water Condensation/Siloxane Hydrolysis:



$$i(i') \in [0, f-1]; \quad j(j') \in [0, f-i(i')].$$

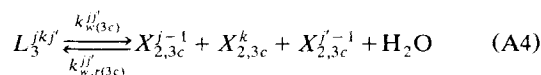
Alcohol Condensation/Siloxane Alcoholysis:



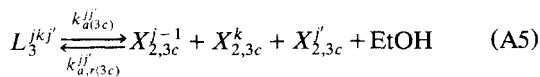
$$i(i') \in [0, f-1]; \quad j \in [0, f-i]; \quad j' \in [0, f-i'-1]$$

where  $X$  is  $M$ ,  $D$ ,  $T$ , or  $Q$ , depending on functionality;  $i$ ,  $i'$  is the number of siloxane bridges attached to site;  $j$ ,  $j'$  is the number of hydroxyl groups attached to site;  $f$  is the functionality of site (number of hydrolyzable groups) and rate coefficients are defined *per mole of reacting group*, not per mole of sites.

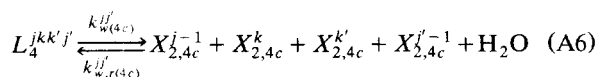
In addition to these general site reaction equations, we also consider unimolecular cyclization reactions of linear oligomers. If  $L_3^{jkj'}$  represents a linear trimer consisting of sites  $X_1^j - X_2^k - X_3^{j'}$  and  $L_4^{jk'j'}$  represents the linear tetramer made up of sites  $X_1^j - X_2^k - X_3^{j'} - X_4^{j'}$ , then the condensation reactions of these linear segments may be written



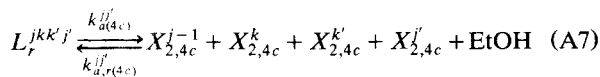
$$j, j' \in [1, f-1]; \quad k \in [0, f-2]$$



$$j \in [1, f-1]; \quad j' \in [0, f-2]$$



$$j, j' \in [1, f-1]; \quad k, k' \in [0, f-2]$$



$$j \in [1, f-1]; \quad k, k', j' \in [0, f-2].$$

We have shown (Sanchez et al., 1996) that when no cyclization occurs, the differential equations describing reactions A1–A3 can be reduced to a set of equations for  $\{[X_i]\}$  and  $\{\langle j \rangle_i\}$ , where

$$[X_i] = \sum_{j=0}^{f-i} [X_i^j]$$

and

$$\langle j \rangle_i = \frac{\sum_{j=0}^{f-i} j [X_i^j]}{[X_i]} = (f-i) \chi_i.$$

Similarly, it can be shown that Eqs. A4–A7 reduce to analogous equations in terms of  $\{[L_3], [L_4]\}$  and  $\{\langle j \rangle_i\}$ , where

$$[L_3] = \sum_{j=\phi}^{f-1} \sum_{k=0}^{f-2} \sum_{j'=0}^{f-1} [L_3^{ijkj'}]$$

and

$$[L_4] = \sum_{j=0}^{f-1} \sum_{k=0}^{f-2} \sum_{k'=0}^{f-2} \sum_{j'=0}^{f-1} [L_4^{jkk'j'}].$$

Presuming that hydrolysis is at pseudoequilibrium and that all condensation reactions are irreversible (with the exception of the closure of the cyclic trimer, as discussed in the body of the article), the full set of differential equations representing the evolution of Scheme 2 is

$$\frac{d[X_0]}{dt} = -\hat{C}_0[X_0] \quad (\text{A8a})$$

$$\begin{aligned} \frac{d[X_1]}{dt} = & \hat{C}_0[X_0] - \hat{C}_1[X_1] - 2(f-1)^2 \overline{k_{\text{eff}(3c)}} [L_3] \\ & + \frac{2}{3} \overline{k_{\text{eff},r(3c)}} [X_{2,3c}] [\text{H}_2\text{O}] - 2(f-1)^2 \overline{k_{\text{eff}(4c)}} [L_4] \end{aligned} \quad (\text{A8b})$$

$$\begin{aligned} \frac{d[X_2]}{dt} = & \hat{C}_1[X_1] - (f-1)^2 \overline{k_{\text{eff}(3c)}} [L_3] \\ & + \frac{1}{3} \overline{k_{\text{eff},r(3c)}} [X_{2,3c}] [\text{H}_2\text{O}] - 2(f-i)^2 \overline{k_{\text{eff}(4c)}} [L_4] \end{aligned} \quad (\text{A8c})$$

$$\frac{d[X_{2,3c}]}{dt} = 3(f-1)^2 \overline{k_{\text{eff}(3c)}} [L_3] - \overline{k_{\text{eff},r(3c)}} [X_{2,3c}] [\text{H}_2\text{O}] \quad (\text{A8d})$$

$$\frac{d[X_{2,4c}]}{dt} = 4(f-1)^2 \overline{k_{\text{eff}(4c)}} [L_4] \quad (\text{A8e})$$

$$\frac{d[L_2]}{dt} = \frac{1}{2} f^2 \overline{k_{\text{eff}(0,0)}} [X_0]^2 - 2\hat{C}_1[L_2] \quad (\text{A8f})$$

$$\begin{aligned} \frac{d[L_3]}{dt} = & 2f(f-1) \overline{k_{\text{eff}(0,1)}} [L_2] [X_0] - 2\hat{C}_1[L_3] \\ & - (f-1)^2 \overline{k_{\text{eff}(3c)}} [L_3] + \frac{1}{3} \overline{k_{\text{eff},r(3c)}} [X_{2,3c}] [\text{H}_2\text{O}] \end{aligned} \quad (\text{A8g})$$

$$\begin{aligned} \frac{d[L_4]}{dt} = & 2f(f-1) \overline{k_{\text{eff}(0,1)}} [L_3] [X_0] + 2(f-1)^2 \overline{k_{\text{eff}(1,1)}} [L_2]^2 \\ & - 2\hat{C}_1[L_4] - (f-1)^2 \overline{k_{\text{eff}(4c)}} [L_4] \end{aligned} \quad (\text{A8h})$$

Some new notation requiring explanation has been introduced in Eq. A8. First, condensation operators have been defined:

$$\hat{C}_i = (f-i) \sum_{i'=0}^{f-1} (f-i') \overline{k_{\text{eff}(i,i')}} [X_{i'}]. \quad (\text{A9})$$

These operators, when applied to  $[X_i]$ , conveniently represent the rate of consumption of that site by bimolecular reactions with all other sites. Also,  $[L_2]$  has been introduced to represent the total concentration of dimers.

In Eqs. A8, *effective* rate coefficients  $\overline{k_{\text{eff}(i,i'')}}$  are the rate coefficients actually measured in a single kinetic experiment. To clarify their meaning, they can be written first in terms of averaged water- and alcohol-producing rate coefficients (e.g.,  $\overline{k_{w(i,i'')}}$  is the averaged forward water-producing condensation rate coefficient):

$$\begin{aligned} \overline{k_{\text{eff}(i,i')}} = & \overline{k_{w(i,i')}} \chi_i \chi_{i'} + \overline{k_{a(i',i)}} \chi_{i'} (1 - \chi_i) \\ & + (1 - \delta_{ii'}) \overline{k_{a(i,i')}} \chi_i (1 - \chi_{i'}) \end{aligned} \quad (\text{A10a})$$

$$\overline{k_{\text{eff}(3c)}} = \overline{k_{w(3c)}} \chi_1^2 + \overline{k_{a(3c)}} \chi_1 (1 - \chi_1) \quad (\text{A10b})$$

$$\overline{k_{\text{eff},r(3c)}} = \overline{k_{w,r(3c)}} + \overline{k_{a,r(3c)}} K_{h,1} \frac{(1 - \chi_1)}{\chi_1} \quad (\text{A10c})$$

$$\overline{k_{\text{eff}(4c)}} = \overline{k_{w(4c)}} \chi_1^2 + \overline{k_{a(4c)}} \chi_1 (1 - \chi_1), \quad (\text{A10d})$$

where the Kronecker delta function ( $\delta_{ii'}$ ) is included to avoid overcounting. Notice that effective rate coefficients are defined as the rate of reaction *per uncondensed group*.

These averaged coefficients were used previously (Sanchez et al., 1996), but here we explicitly describe the averaging:

$$\overline{k_{w(i,i')}} = \sum_{j=1}^{f-i} \sum_{j'=1}^{f-i'} \frac{k_{wij'}^{jj'} (j' [X_i^j] [X_{i'}^{j'}])}{\langle j \rangle_i \langle j' \rangle_{i'} [X_i] [X_{i'}]} \quad (\text{A11a})$$

$$\overline{k_{a(i,i')}} = \sum_{j=1}^{f-i} \sum_{j'=0}^{f-i'-1} \frac{k_{aii'}^{jj'} \{j(f-i'-j') [X_i'] [X_{i'}']\}}{\langle j \rangle_i (f-i'-\langle j \rangle_{i'}) [X_i] [X_{i'}]} \quad (\text{A11b})$$

$$\overline{k_{w(3c)}} = \sum_{j=1}^{f-1} \sum_{j'=0}^{f-1} \sum_{k=0}^{f-2} \frac{k_{w(3c)}^{jj'} (j' [L_3^{jkj'}])}{\langle j \rangle_1^2 [L_3]} \quad (\text{A11c})$$

$$\overline{k_{a(3c)}} = \sum_{j=1}^{f-1} \sum_{j'=0}^{f-2} \sum_{k=0}^{f-2} \frac{k_{a(3c)}^{jj'} \{j(f-1-j') [L_3^{jkj'}]\}}{\langle j \rangle_1 (f-1-\langle j \rangle_1) [L_3]} \quad (\text{A11d})$$

$$\overline{k_{w,r(3c)}} = \sum_{j=0}^{f-2} \sum_{j'=0}^{f-2} \frac{k_{w,r(3c)}^{jj'} [X_{2,3c}^j] [X_{2,3c}^{j'}]}{[X_{2,3c}]^2} \quad (\text{A11e})$$

$$\overline{k_{a,r(3c)}} = \sum_{j=0}^{f-2} \sum_{j'=0}^{f-2} \frac{k_{a,r(3c)}^{jj'} [X_{2,3c}^j] [X_{2,3c}^{j'}]}{[X_{2,3c}]^2} \quad (\text{A11f})$$

$$\overline{k_{w(4c)}} = \sum_{j=1}^{f-1} \sum_{j'=1}^{f-1} \sum_{k=0}^{f-2} \sum_{k'=0}^{f-2} \frac{k_{w(4c)}^{jj'} (j' [L_4^{jkk'j'}])}{\langle j \rangle_1^2 [L_4]} \quad (\text{A11g})$$

$$\overline{k_{a(4c)}} = \sum_{j=1}^{f-1} \sum_{j'=0}^{f-2} \sum_{k=0}^{f-2} \sum_{k'=0}^{f-2} \frac{k_{a(4c)}^{jj'} \{j(f-1-j') [L_4^{jkk'j'}]\}}{\langle j \rangle_1 (f-1-\langle j \rangle_1) [L_4]} \quad (\text{A11h})$$

Now that the effective condensation-rate coefficients have been well defined in terms of the individual rate coefficients in reactions A2–A7, the effects of changing water content can be understood clearly. Assuming that condensation reactivity is independent of the degrees of hydrolysis of the reacting sites, the averaging in Eq. A11 becomes unnecessary. However, changing water content changes the fractional extents of hydrolysis observed at pseudoequilibrium  $\{\chi_i\}$ . Equation A10 demonstrates that this will change the relative contributions of alcohol and water condensation of the effective rate coefficients. In the absence of other effects of changing water, this means that the average water and alcohol condensation rate coefficients can be separated by varying water content. Assink and Kay have used this technique to ascer-

tain the roles of alcohol- and water-producing dimerization. Both mechanisms play a role for tetramethoxysilane (especially at low water content) (Assink and Kay, 1988a), but alcohol-producing dimerization can be neglected under most conditions for tetraethoxysilane (Assink and Kay, 1993).

We are investigating the effects of water content on methylethoxysilanes in more detail, but here we tentatively discuss trends in terms of water-producing rate coefficients found by normalizing the effective rate coefficient by the fractional extents of hydrolysis of reacting sites. By doing this, we can compare reactivities of different sites on a consistent basis (per silanol group) when the number of possible groups per site changes. Note, however, that Eq. A10 allows one to recover the effective rate coefficients or to see how the trends would change if alcohol-producing condensation were assumed to dominate instead of water-producing. Since differently connected sites have similar fractional extents of hydrolysis, the assumption about the actual condensation route does not change the nature of the reported trends.

Note that Eqs. A8 have been stated in their most complete form for a difunctional monomer. The model should not be used to analyze data for nonlinear monomer systems once branched sites appear. Cyclization can be neglected by removing the relevant cyclization terms in those equations [recovering the model used previously (Sanchez et al., 1996)]. For the monofunctional system (and for any system at the very earliest conversion), only dimerization need be considered, in which case only the simple analytical solution is needed:

$$\frac{1}{[X_0]} = \frac{1}{[X_0]_0} + \overline{k_{\text{eff}(0,0)}} t$$

where

$$t \in \{t: \langle j \rangle_0 \approx \langle j \rangle_{0,\text{eq}}; [X_{i>1}] \approx 0\}. \quad (\text{A12})$$

Manuscript received July 9, 1997, and revision received Feb. 11, 1998.